TNO PUBLIC



Westerduinweg 3 1755 LE Petten P.O. Box 15 1755 ZG Petten The Netherlands

www.tno.nl

T +31 88 866 50 65

TNO report

TNO 2018 R10762

Verification of ZephIR 300 unit 315 at ECN part of TNO LiDAR Calibration Facility, for offshore measurements at Euro Platform (EPL)

Date March 2019

Author(s) D.A.J. Wouters and J.P. Verhoef

Copy no No. of copies

Number of pages 64 (incl. appendices)

Number of appendices 2

Sponsor Dutch ministry of Economic Affairs and Climate Policy

Project name 2018 Wind conditions @ North Sea

Project number 060.33997

All rights reserved.

No part of this publication may be reproduced and/or published by print, photoprint, microfilm or any other means without the previous written consent of TNO.

In case this report was drafted on instructions, the rights and obligations of contracting parties are subject to either the General Terms and Conditions for commissions to TNO, or the relevant agreement concluded between the contracting parties. Submitting the report for inspection to parties who have a direct interest is permitted.

© 2019 TNO

Management Summary

Verification of ZephIR 300 unit 315 Title

at ECN part of TNO LiDAR Calibration Facility,

for offshore measurements at Euro Platform (EPL)

: D.A.J. Wouters and J.P. Verhoef Author(s)

: March 2019 Date

ECN beschikkingsbrief EZK, 2018TNO 2018 R10762 Order nr.

Report nr.

Revision

Rev.	Date	Description
0.1	06-2018	Initial draft
1.2	03-2019	Release

Archiving

\\tsn.tno.nl\RA-Data\Express\Wind-op-Zee









RvA is participant in the ILAC MRA.

ECN part of TNO Wind Energy is accredited conform ISO / IEC 17025 and accepted as RETL under IECRE WE-OMC.

- Power performance measurements according to IEC 61400-12-1, Measnet Power Performance measurement procedure, FGW TR2, FGW TR5
- NTF/NPC measurements according to IEC 61400-12-2
- Mechanical loads measurements according to IEC 61400-13
- Meteorological parameters (windspeed, wind direction, temperature, air pressure, relative humidity conform IEC 61400-12-1)
- Characterization of Remote Sensing Devices conform IEC 61400-12-1, Appendix L

Results only apply for the tested LiDAR with the settings used during the measurement period.

In case copies of this report are made, only integral copying is allowed.

Summary

As part of the North Sea offshore wind conditions measurement program a ZephIR LiDAR is installed at Euro Platform on 2 August 2018. In order to assure high quality measurements, the LiDAR unit (ZephIR 300, 315) was validated at the ECN part of TNO LiDAR Calibration Facility for the period of 24 April 2018 13:00 until 07 June 2018 10:00. ECN part of TNO is ISO 17025 accredited for remote sensing device calibration, where the Meteorological Mast 4 measurements are in accordance with IEC 61400-12-1:2015, Annex G and the LiDAR verification in accordance with IEC 61400-12-1:2017, Annex L. The validation is performed by checking Key Performance Indicators.

The comparison of the LiDAR against the Meteorological Mast 4 is performed for 5 measurement heights: 29 m, 44 m, 59 m, 90 m and 100 m and the results for the validation and verification analyses are summarized in the tables below (see also tables 1 and 3).

KPI	height	result	unit	lower limit	upper limit	status
	m	unit		unit	unit	
	100	0.990	-			pass
	90	0.997	-			pass
$slope_{WS,1p}$	59	0.986	-	0.98	1.02	pass
	44	0.990	-			pass
	29	0.984	-			pass
	100	0.999	-			pass
	90	0.999	-			pass
$R^2_{WS,1p}$	59	1.000	-	0.98		pass
, .	44	1.000	-			pass
	29	0.999	-			pass
	100	3.470	0			pass
	90	3.442	0			pass
offset _{WD,median}	59	3.976	0	-5	5	pass
	44	2.889	0			pass
	29	3.624	0			pass
	100	0.437	%			pass
	90	1.029	%			pass
$\Delta_{90_{WD}}$	59	1.025	%		3	pass
	44	0.927	%			pass
	29	0.881	%			pass

height	slope	offset	R^2
m	-	m/s	
100	0.990	0.007	0.999
90	1.000	-0.038	0.999
59	0.982	0.038	1.000
44	0.981	0.094	1.000
29	0.970	0.132	1.000

A sensitivity analysis is performed for the LiDAR. Significant sensitivities were found for the environmental variables: relative humidity, wind veer and wind shear. The results are shown in the table below (see also table 14). Relative humidity has the highest influence on the accuracy.

environmental variable	comparison height			overall		
	100 m	90 m	59 m	44 m	29 m	
shear exponent					✓	√
turbulence intensity						
precipitation						
wind direction						
air temperature						
relative humidity	✓	\checkmark	\checkmark	\checkmark	✓	✓
air density						
flow inclination						
wind veer			✓	✓	✓	✓
reference wind speed						

Based on these results ECN part of TNO qualifies this LiDAR unit as suitable for offshore application at Euro Platform.

Contents

	wanagement Summary	2
	Summary	4
	List of tables and figures	7
1	Introduction	9
2	Measurement campaign	10
2.1	ECN part of TNO LiDAR Calibration Facility	10
2.2	Meteorological mast	
2.3	LiDAR	
2.4	Measurement sector	13
2.5	Data stream	
3	Data preparation	15
4	LiDAR Validation KPIs	16
4.1	Wind speed comparison	16
4.2	Wind direction comparison	
4.3	Availability	
5	LiDAR Verification	21
5.1	Direct data comparison	21
5.2	Bin-wise data comparison	
5.3	Systematic uncertainties	
5.4	Environmental conditions	
6	Sensitivities	39
6.1	Sensitivity analysis	39
6.2	Impact on accuracy	40
7	Uncertainty	
7.1	Reference devices - cup anemometers	
7.2	Remote sensing device	47
8	Deviations	49
9	References	50
10	Signature	51
	Appendices	52
Α	IEC visualisations	52
В	Instrumentation details	57
B.1	Calibration sheets	62
	Nomenclature	61

List of tables and figures

1 2	LiDAR validation Key Performance Indicators results LiDAR availability KPIs	
3 4 5 6 7 8 9 10 11 12	LiDAR verification IEC 61400-12-1 Annex L results Uncertainty calculations of the rsd @29 m. Uncertainty calculations of the rsd @44 m. Uncertainty calculations of the rsd @59 m. Uncertainty calculations of the rsd @90 m. Uncertainty calculations of the rsd @100 m. Environmental conditions @29 m. Environmental conditions @44 m. Environmental conditions @59 m. Environmental conditions @59 m. Environmental conditions @90 m.	29 30 31 32 33 34 35 36 37
13 14 15 16 17	Overview of significant sensitivities Preliminary accuracy classes Parameters derived from the sensitivity analysis of the rsd. Maximum influence of environmental variables on the rsd.	41 41 43
18 19 20 21	Signals used for each comparison heights List of measured signals List of equipment used per signal List of calculated (pseudo) signals	59 60
Figui	res	
1 2 3 4 5	Overview of the EWTW ZephIR 300, unit 315 at the ELCF Position of the LiDAR relative to MM4. Ground level elevation map of the LiDAR's surroundings Measurement sector.	12 13
6 7 8 9 10	Comparison of 10-minute averages of the wind direction @29 m	19 19 20
11 12 13 14 15 16 17 18 19	Wind speed comparison @29 m Wind speed comparison @44 m Wind speed comparison @59 m Wind speed comparison @90 m Wind speed comparison @100 m Bin-wise wind speed comparison @29 m Bin-wise wind speed comparison @44 m Bin-wise wind speed comparison @59 m Bin-wise wind speed comparison @90 m Bin-wise wind speed comparison @90 m	23 24 24 24 25 25 25 26
21 22 23	Environmental conditions: shear exponent	27

24	Air temperature @96m	52
25	Influence of the wake of MM4 on the LiDAR	53
26	Contributions to the LiDAR uncertainty	54
27	Histograms for bin-wise wind speed comparison	55
28	Significant LiDAR sensitivities	56
29	Layout of Meteorological Mast 4	58

1 Introduction

The Dutch government has ambitious plans for offshore wind energy towards 2020 and beyond. In order to achieve the goals that have been set, various development zones have been defined in the North Sea. The Dutch government creates a level playing field for developers among others to provide them with wind data on which business cases can be build.

To acquire wind data, the Dutch ministry of Economic Affairs and Climate Policy has contracted ECN Wind Energy to carry out a measurement campaign on the North Sea. This campaign comprises among others of LiDAR measurements at Lichteiland Goeree (LEG), Euro Platform (EPL) and K13-A. To this end, the ZephIR 300 LiDAR 315 was installed at EPL on 2 August 2018.

High quality measurements will reduce the uncertainty in the measurements creating more favourable finance conditions for developers. Therefore, and to assure the high quality, the LiDAR was first verified and validated at the ECN part of TNO LiDAR Calibration Facility (ELCF) [1] located at the ECN Wind Turbine test site Wieringermeer (EWTW).

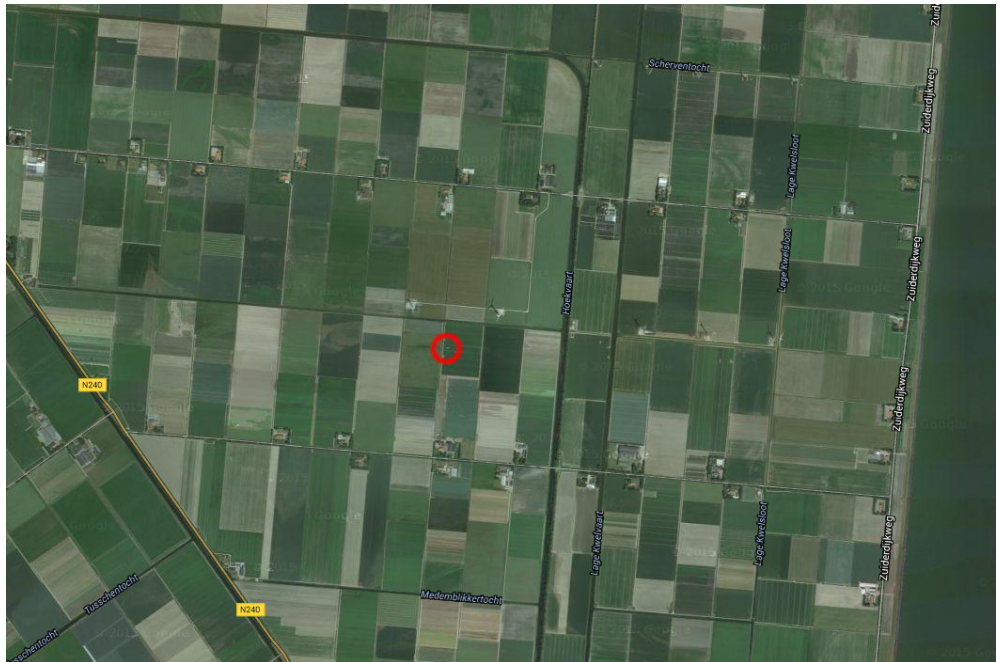
This report describes the comparison of the LiDAR with Meteorological Mast 4 (MM4) for the period of 24 April 2018 13:00 until 07 June 2018 10:00. The measurements at the mast are performed in accordance with IEC 61400-12-1:2005 [2]. Furthermore, the LiDAR is validated and verified, where validated means that Key Performance Indicators (KPIs) are checked. These KPIs are set up by ECN part of TNO based on NORSEWinD criteria [3] and the 'Carbon Trust Offshore Wind Accelerator roadmap for the commercial acceptance of floating LIDAR technology' [4]; they are defined in chapter 4. The verification is done in accordance with Annex L of IEC 61400-12-1:2017 [5].

The measurement campaign is described in chapter 2 and details the site, the mast and the LiDAR. It focuses on Meteorological Mast 4; a full description of the calibration facility can be found in the instrumentation report [1]. Chapter 3 describes the data preparation steps. The validation of the KPI's is discussed in chapter 4 and the verification analysis results are presented in chapter 5. In addition, a sensitivity analysis is presented in chapter 6. Chapters 7 and 8 present the uncertainty analysis and deviations with respect to the standards applied.

2 Measurement campaign

2.1 ECN part of TNO LiDAR Calibration Facility

The ECN part of TNO LiDAR Calibration Facility (ELCF) is part of the ECN Wind Turbine test site Wieringermeer (EWTW). The site mainly consists of agricultural land, with single farmhouses and rows of trees as shown in fig. 1. It is located in the Wieringermeer, a polder in the north east of the province of North Holland, 3 km north of the village of Medemblik. To the east, the site is 1 km removed from the vast lake IJsselmeer. The altitude is 5 m below sea level. The site is considered flat terrain according to IEC 61400-12-1:2017 [5].



Source: Google Maps

Figure 1: Overview of the EWTW; highlighted in red is the location of the ECN LiDAR Calibration Facility

2.2 Meteorological mast

The ELCF is detailed in a separate report [1]. The Meteorological Mast 4 is an essential part of the ELCF. It is a 100 m tall lattice tower with a triangular cross section, supported by guy wires at two levels: 41 m and 83 m. The guy wires are fixed to concrete anchors at a radius of 60 m from the tower base at 95°, 215° and 335°.

The MM4 and its sensors are detailed in appendix B. The wind speed is measured at 29 m, 44 m, 59 m, 90 m and 100 m. These are the heights at which the LiDAR measurements are compared to the MM4. The comparison heights are detailed in table 18.

At the heights of 87.5 m and 42 m multiple sensors are installed on two or three booms of MM4. By combining the signals from these sensors, the influence of the mast on the measurements can be minimized. The resulting signal is an example of what is referred to as a 'pseudo signal'. All pseudo signals are defined in table 21. At 100 m two closely spaced anemometers are mounted accompanied by two vanes at 97 m. At 87.5 m two booms are installed, which measure the wind speed at 90 m and the

wind direction at 88 m. At 42 m three booms are installed, which measure the wind speed at 44 m and the wind direction at 42 m. The layout of MM4 is shown in fig. 29.

All wind speed measurements are performed with Thies First Class Advanced cup anemometers. All wind direction measurements use Thies First Class wind vanes. The full instrumentation applicable for this report is listed in table 19. The sensors and data acquisition modules used are detailed in table 20.

The cup anemometers and wind vanes on MM4 are calibrated on a yearly basis, i.e. one year after the installation date. All instruments and data acquisition modules are calibrated according to internal procedures. Calibration certificates are available at the ECN offices in Petten. The latest calibration certificates of one of the topmost cups and vanes used are presented in appendix B.

2.3 LiDAR

The LiDAR is a ZephIR 300. This unit has identification number 315. Using Waltz 4.60 with the ZPH files produced by the LiDAR, its firmware version is found to be 2.1027. According to the LiDAR configuration extracted from the CSV files, produced from the ZPH files using Waltz, the LiDAR (shown below), it is configured to perform measurements at ten heights: 29 m, 44 m, 59 m, 90 m, 100 m, 120 m, 140 m, 160 m, 180 m and 200 m. Note that the configured measurement heights are measured above the ZephIR window, which is 1 m above the ground. The measurement height of 38 m above the lens is a default, non-configurable measurement height. The LiDAR has a cone half-angle of 30.0°. A picture of the 300 315 LiDAR deployed at the ECN part of TNO LiDAR Calibration Facility during the verificiation test is presented in fig. 2.

CSV Converter: v1.209
Filter: v1.040
Averager: v1.2
File system version: v5
Unit: 315
Time sync: UTC +0 hrs
Time stamps indicate the beginning of the averaging period
38m is a fixed reference measurement
The GPS field contains latitude and longitude coordinates in decimal degrees (positive sign indicates North or East)
ZephIR window height above ground: 1.0m
Measurement heights: 199m 179m 159m 139m 119m 99m 89m 58m 43m 38m 28m

To achieve the highest quality LiDAR measurements, a filter named 'availability' is defined based on the number of packets logged for each 10-minute averaged sample. In order to quantify the overall availability of the LiDAR in a 10-minute interval (for a certain height), we normalize the number of packets in a 10-minute interval to 100 % using

availability =
$$\frac{n_{\mathsf{packets}}}{\mathsf{max}(n_{\mathsf{packets}})} \cdot 100 \,\%$$
 (2.1)

where $\max(n_{\text{packets}})$ is the maximum value for the number of packets metric observed in the entire data set.

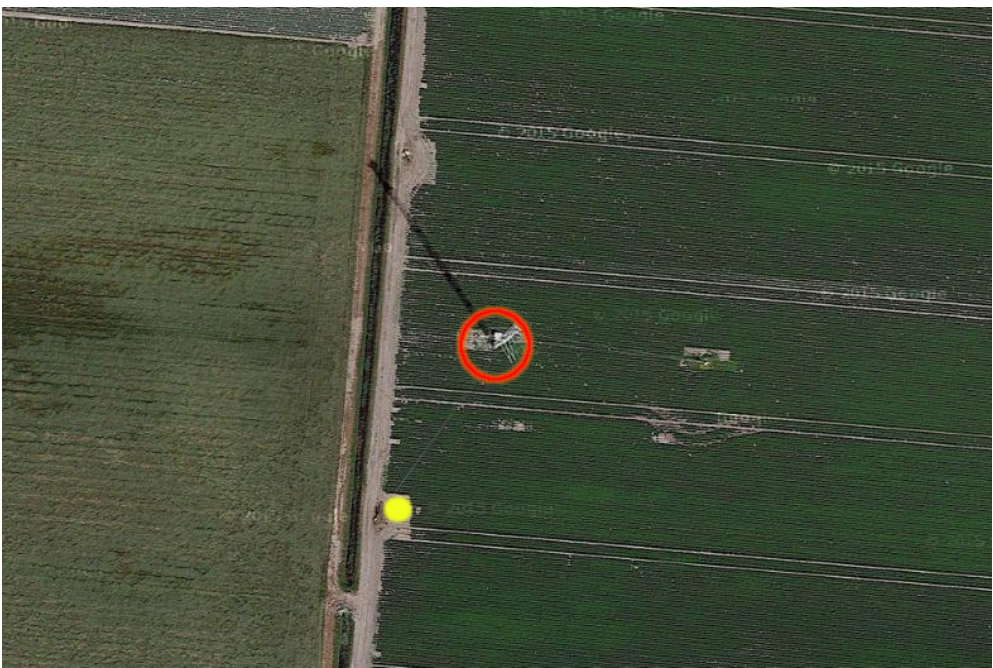


Photo by Gerben Bergman

Figure 2: ZephIR 300, unit 315 (front center, labeled *ECN*) at the ECN part of TNO LiDAR Calibration Facility next to the guy wire anchor of Meteorological Mast 4

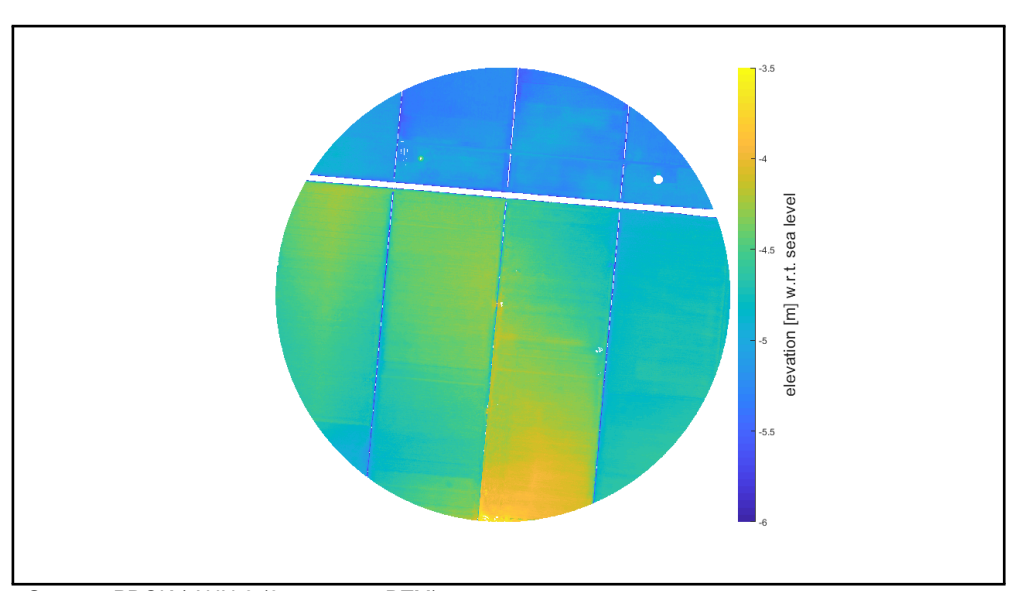
2.4 Measurement sector

As part of the ELCF a dedicated platform for placing remote sensing equipment is created near the anchor of the 215° guy wires, as shown in fig. 3. The area surrounding the LiDAR platform is very flat as demonstrated by the laser altimetry in fig. 4.



Source: Google Maps

Figure 3: Position of the LiDAR relative to MM4; indicated in red is the Meteorological Mast 4 and in yellow the calibration platform



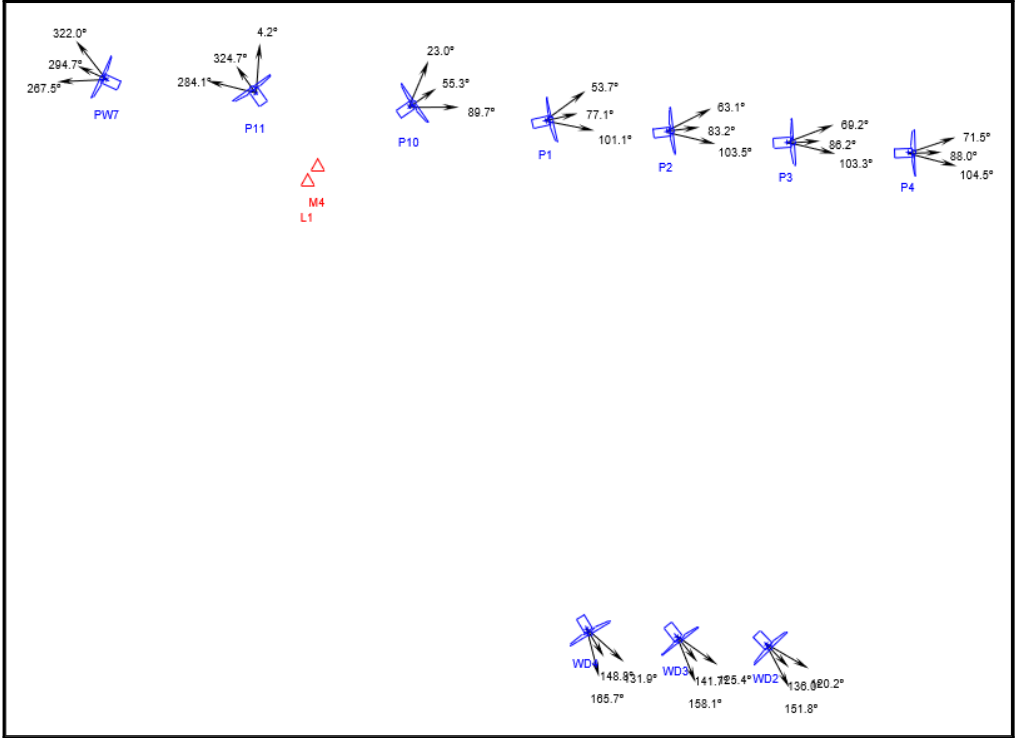
Source: PDOK / AHN-3 (0.5 m raster DTM)

Figure 4: Ground level elevation map of the LiDAR's surroundings (radius = $5 \times 100 \, \text{m}$)

The wind direction sector for which the measurements of both the mast and the LiDAR are unaffected by obstacles is referred to as the measurement sector. It is determined using Meassector 2.2.1 [6]. The objects affecting the measurement sector are shown in fig. 5. Figures 4 and 5 use the same grid map (RD-coordinates). All angles are relative to the grid North.

The total measurement sector is composed of the following sectors.

- 4.2° to 23.0°
- 104.5° to 120.1°
- 165.7° to 267.4°



Source: Meassector 2.2.1

Figure 5: Measurement sector. Total excluded sector per obstacle.

2.5 Data stream

The Meteorological Mast 4 is connected via a glass fibre network to the measurement office on the test site. From here, the data are transported on a daily basis to the offices in Petten, where they are stored in a dedicated Wind Data Management System (WDMS) database [7].

The LiDAR data are accumulated in the LiDAR device itself. The data files are transferred directly to the offices in Petten. The binary files are converted to ASCII using ZephIR Waltz, Version 4.60.

Valid data are gathered from 24 April 2018 13:00 until 07 June 2018 10:00. All times are expressed in UTC.

3 Data preparation

The validation, verification and sensitivity analyses are performed using 10 minute average values. The following data filters are applied at each comparison height, in accordance with Annex L.2.3 [5].

a) Mast free of wake from obstacles

The measurement sector is defined in section 2.4 and the filtering is applied to the wind direction measurements at each comparison height individually.

b) LiDAR probe volumes free of wake from obstacles

The measurement sector ensures the LiDAR is not in the wake of any obstacles. However, the LiDAR could be affected by the wake of the MM4.

The LiDAR is located 60 m from the base of MM4. For this analysis the probe volumes are represented by the entire conical measurement volume. At all measurement heights Meteorological Mast 4 is outside the (circular) measurement volume of the LiDAR. Due to the cone angle of the LiDAR, the radius of this circle increases with measurement height. The potential interference of the wake of MM4 on the LiDAR, is visualised in fig. 25. These figures show the ratio of the wind speeds measured by MM4 and the LiDAR for each comparison height. The bin-wise average wind speed ratios where the LiDAR is in the wake of the MM4 do not differ significantly from the ratio in the undisturbed sector. Therefore, we do not apply any filtering.

c) Anemometers free of wake from mast

The influence of the MM4 wake on the reference cup anemometers is mitigated by using multiple cups on booms at different angles at most measurement heights, combined with the pseudo signal equations listed in table 21. At comparison height 59 m only a single boom is present. In this case the additional sector of 310° to 360° is omitted for the wind speed measurements at this comparison height. The filtering performed is based on the wind direction measured by the wind vane installed at this comparison height. This filtering has no influence on the data, because the sector 310° to 360° is not part of the measurement sector.

d) Cup anemometers free of icing

To eliminate the influence of icing on the wind speed measurements, the MEASNET icing criterion is used. All data acquired by cup anemometers is disregarded if the air temperature, measured at 96 m is lower than 2 °C while the relative humidity is higher than 80 %. The time series of the recorded air temperature is shown in fig. 24.

e) LiDAR availability

All data with LiDAR availability less than 90 % are filtered from the data set. The availability is derived as the ratio of the amount of packets registered in a 10-minute interval and the observed maximum number of packets (39).

f) Precipitation

As prescribed by IEC 61400-12-1, no filtering is performed on precipitation.

4 LiDAR Validation KPIs

For each comparison height, the 10-minute averaged wind speed and wind direction measured by the LiDAR are compared to the values obtained with the sensors on the Meteorological Mast 4. We will refer to the LiDAR results as 'rsd' (remote sensing device) and the Meteorological Mast 4 results as 'ref' (reference).

Regression parameters of the wind speed and direction comparisons are identified as Key Performance Indicators (KPIs), which should lie in specified ranges. This is referred to as LiDAR validation and results are presented in this chapter.

4.1 Wind speed comparison

The wind speed plots in figs. 11 to 15 show the raw data, which are the 10-minute averaged wind speed samples, in blue. The deviation, in red, is the relative difference between the wind speeds measured by the ref, $v_{\rm ref}$, and the rsd, $v_{\rm rsd}$. The deviation is defined as

$$deviation = \frac{v_{rsd} - v_{ref}}{v_{ref}} \cdot 100 \%$$
 (4.1)

From the raw data, bin-wise mean values are computed, which are represented by square markers. The bin-width equals $0.5\,\mathrm{m/s}$, centred at integer multiples of $0.5\,\mathrm{m/s}$. The first and last bin are only $0.25\,\mathrm{m/s}$ wide to fill the $4\,\mathrm{m/s}$ to $16\,\mathrm{m/s}$ range. The bin-wise mean values of bins that do not meet the bin-count threshold of three samples are omitted.

Two regression methods are applied to the data. The two-parameter (2p) method, a linear regression using a slope and offset, is applied to both the raw data and the bin-wise means (binmeans).

$$y_{2p} = \mathsf{slope} \cdot x + \mathsf{offset}$$

The one-parameter (1p) method, a linear regression using only a slope that passes through the origin, is applied to the bin-wise means only.

$$y_{1p} = \mathsf{slope} \cdot x$$

The regression results are shown in the wind speed plots. In these figures the $y_{bin,1p}$ results, which are used as a validation KPI, agree well with the IEC prescribed $y_{bin,2p}$ results, which will be discussed in chapter 5.

4.2 Wind direction comparison

Performing a regression on the wind direction comparison which features a slope - as was done for the wind speed - makes little physical sense, because the value obtained at 0° should match the one at 360°. Therefore, we only consider the offset. This is best visualised by plotting the difference.

The wind direction comparison plots in figs. 6 to 10 show the difference between the wind direction measured by the ref, $wd_{\rm ref}$, and the rsd, $wd_{\rm rsd}$. The difference is defined as

$$\Delta_{wd} = wd_{\text{rsd}} - wd_{\text{ref}} \tag{4.2}$$

From the raw data, bin-wise mean values are computed, which are represented by square markers. The bin-width equals 10°. The bin-wise mean values of bins that do

not meet the bin-count threshold of three samples are omitted. The regression of the binmeans is in this case simply the mean of the binmeans.

Strong outliers can be caused by the heterodyne detection, which causes the LiDAR to sometimes report the wind direction with a 180° error. The percentage of the samples affected are reported as $\Delta_{90_{\rm WD}} \equiv |\Delta_{wd}| > 90^{\circ}$. These outliers strongly influence the binmeans (and standard deviation). To provide an estimate of the offset in the unaffected samples, the median value of Δ_{wd} is shown too.

ECN part of TNO has defined KPIs on wind speed and wind direction regression parameters in the same fashion as the NORSEWinD criteria [3] and the KPIs defined in the 'Carbon Trust Offshore Wind Accelerator roadmap for the commercial acceptance of floating LIDAR technology' [4]. The KPIs are shown in table 1. All criteria are met.

KPI	height	result	unit	lower limit	upper limit	status
	m	unit		unit	unit	
	100	0.990	-			pass
$slope_{WS,1p}$	90 59	0.997 0.986	-	0.98	1.02	pass pass
Siopo _{WS,1p}	44	0.990	-	0.00	1.02	pass
	29	0.984	-			pass
	100	0.999	-			pass
\mathbf{p}^2	90	0.999	-	0.00		pass
$R^2_{WS,1p}$	59 44	1.000	-	0.98		pass
	29	0.999	-			pass pass
	100	3.470	0			pass
	90	3.442	0			pass
offset _{WD,median}	59	3.976	0	-5	5	pass
	44	2.889	0			pass
	29	3.624				pass
	100	0.437	%			pass
_	90	1.029	% %		3	pass
$\Delta_{90_{WD}}$	59 44	1.025 0.927	% %		ა	pass
	29	0.881	% %			pass

4.3 Availability

This section presents the LiDAR availability KPIs. We use the KPIs as defined in Offshore Wind Accelerator (OWA) roadmap [4].

The monthly availabilities are reported in table 2 per calendar month. Therefore the first and last month contain the data for a fraction of the month. The monthly system availability (MSA) represents the time that the LiDAR system was recording data. The monthly post-processed data availability (MPDA) represents the time that the LiDAR delivered data that passed our filtering criteria. It should be noted that the MPDA is strongly affected by the lower limit that is chosen for the LiDAR availability metric, which we set to 90 %.

Table 2 also lists the overall system availability and the overall data availability for the whole campaign. Only these overall values are evaluated as a KPI. We require the overall system availability to exceed 90% and the overall data availability to exceed

 $85\,\%$ at each comparison height. The data availability meets these requirements at all comparison heights.

Table 2: LiDAR availability KPIs

month	samples	MSA	MPDA				
			100 m	90 m	59 m	44 m	29 m
		%	%	%	%	%	%
April	930	100.0	80.6	81.0	81.0	81.1	80.8
May	4464	100.0	97.0	97.0	97.0	97.0	97.0
June	924	100.0	95.9	95.8	95.9	95.8	95.8
overall	6318	100.0	94.4	94.5	94.5	94.5	94.4

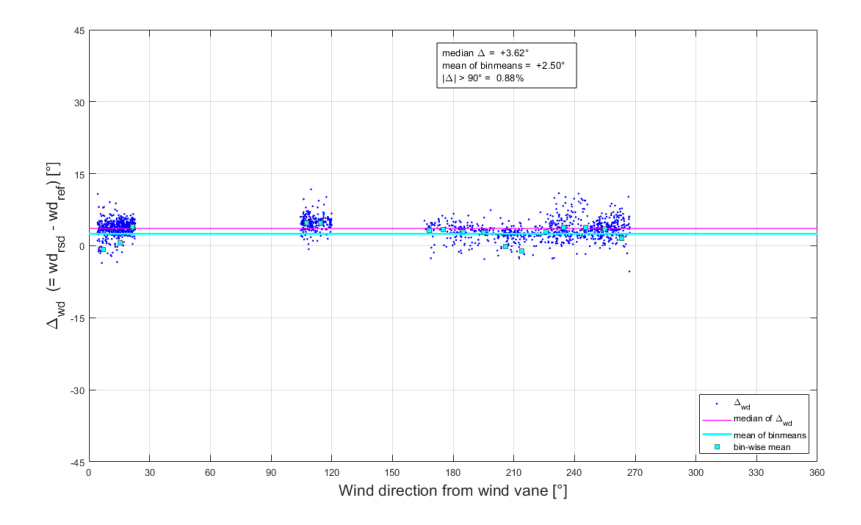


Figure 6: Comparison of 10-minute averages of the wind direction @29 m

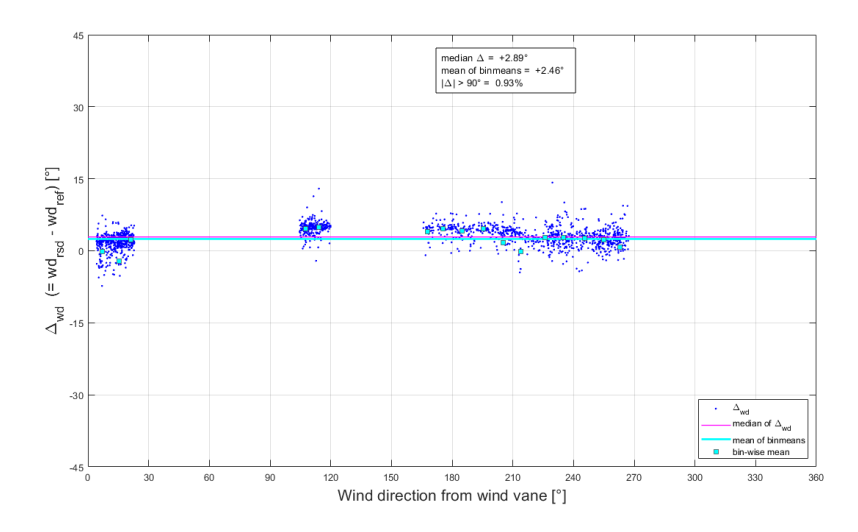


Figure 7: Comparison of 10-minute averages of the wind direction $@44\,\mathrm{m}$

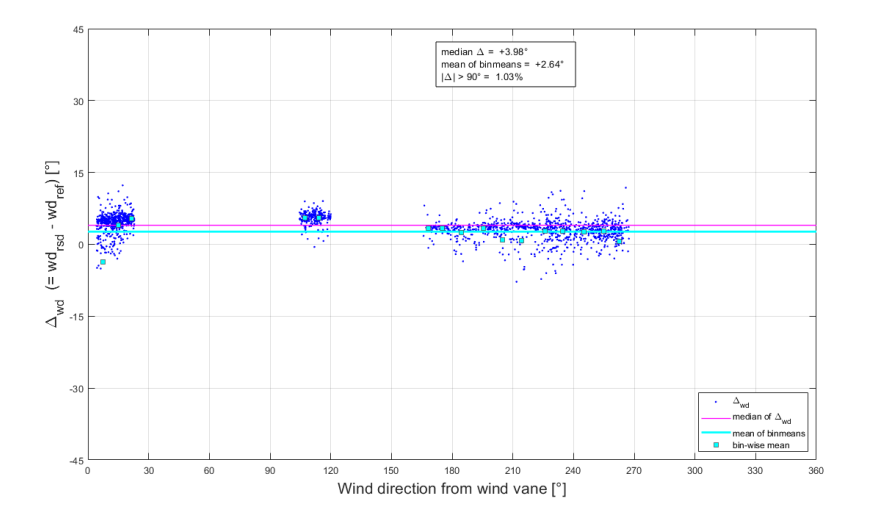


Figure 8: Comparison of 10-minute averages of the wind direction $@59\,\mathrm{m}$

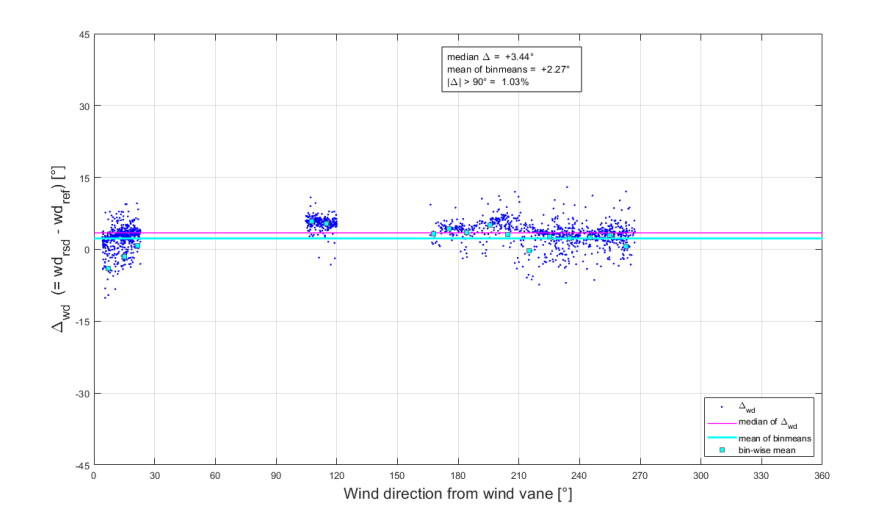


Figure 9: Comparison of 10-minute averages of the wind direction $@90\,\text{m}$

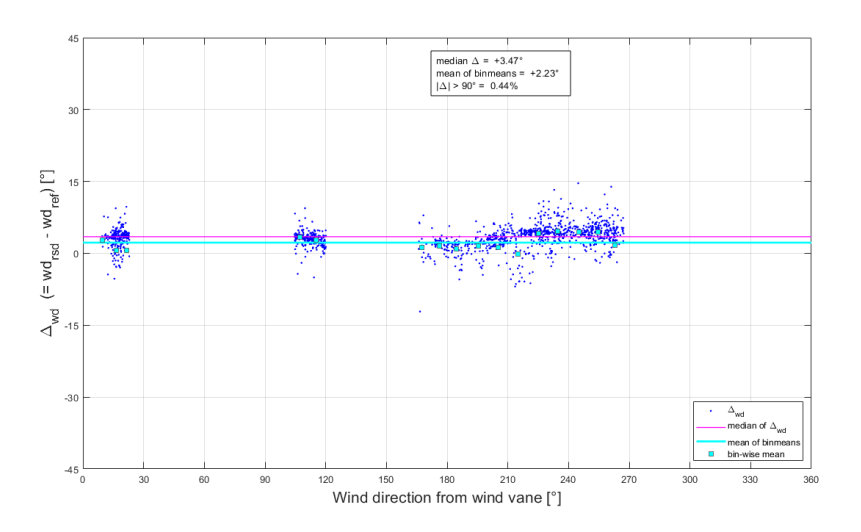


Figure 10: Comparison of 10-minute averages of the wind direction @100 m

5 LiDAR Verification

This chapter reports the results of the LiDAR verification analysis as defined in annex L.3 [5]. The analysis is performed using the in-house software tool *RSDverification* version 1.1.1.

5.1 Direct data comparison

A comparison of the horizontal wind speed between the Meteorological Mast 4 devices and the LiDAR for each comparison height is presented in figs. 11 to 15. The format is taken from figure L.5 [5]. Only samples for which the reference wind speed is in the range of $4 \,\mathrm{m/s}$ to $16 \,\mathrm{m/s}$ are used.

5.2 Bin-wise data comparison

The bin-wise comparison described in Annex L.3 [5] first requires binning of the reference wind speeds measured on the Meteorological Mast 4. The prescribed bin width is $0.5\,\text{m/s}$ centred on integer multiples of $0.5\,\text{m/s}$. Because the range is $4\,\text{m/s}$ to $16\,\text{m/s}$, the first and last bin are given half the prescribed width and are centred at $4.125\,\text{m/s}$ and $15.875\,\text{m/s}$ respectively.

The resulting bin count histograms are presented in fig. 27. Due to the smaller bin width, the first and last bin have a significantly lower bin count.

With the exception of $100\,\text{m}$, all comparison heights have bins in the upper end of the $4\,\text{m/s}$ to $16\,\text{m/s}$ range that contain less than the minimum of three data sets, specified by data coverage requirement c) [5, L.2.2]. This is a deviation from the standard, reported in chapter 8.

The resulting bin-wise comparisons for each measurement height, are presented in figs. 16 to 20. The results of the regressions are summarised in table 3. The uncertainty intervals shown in these figures are discussed in section 7.1.

Table 3: LiDAR verification IEC 61400-12-1 Annex L results

height	slope	offset	R^2
m	-	m/s	
100	0.990	0.007	0.999
90	1.000	-0.038	0.999
59	0.982	0.038	1.000
44	0.981	0.094	1.000
29	0.970	0.132	1.000

5.3 Systematic uncertainties

The results of the systematic uncertainty analysis, as described in section 7.2, are presented for each comparison height in tables 4 to 8. The tables are modelled after table L.9 [5]. The total LiDAR uncertainty is reported in column ' $V_{\rm rsd}$ '.

If there are fewer than three data sets in any bin, all statistics (mean and standard deviation) and derived properties are omitted from the table.

5.4 Environmental conditions

The uncertainty computation for the LiDAR as part of a future power performance campaign requires the environmental conditions experienced during the LiDAR verification test [5, annex L.7.1, item i]. For completeness we report the environmental conditions even though this verification test is not linked to a power performance campaign. The conditions at each comparison height are reported in tables 9 to 13. The environmental data is subject to the same filtering steps as the (wind speed) data used for the verification analysis. The environmental data is binned against the reference wind speed¹.

In addition to the tabulated sensitivity results, these environmental variables for which a significant sensitivity is found in 14 are also plotted as a function of wind speed along with their distribution in figs. 21 to 23.

¹For the reference wind speed the bin centre is reported, because each environmental condition may have a slightly difference bin-wise mean wind speed depending on the availability of environmental data.

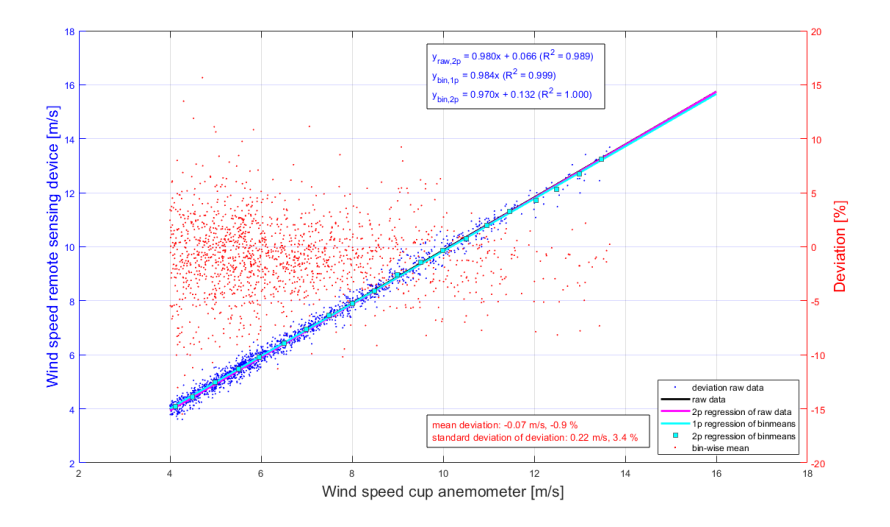


Figure 11: Wind speed comparison @29 m

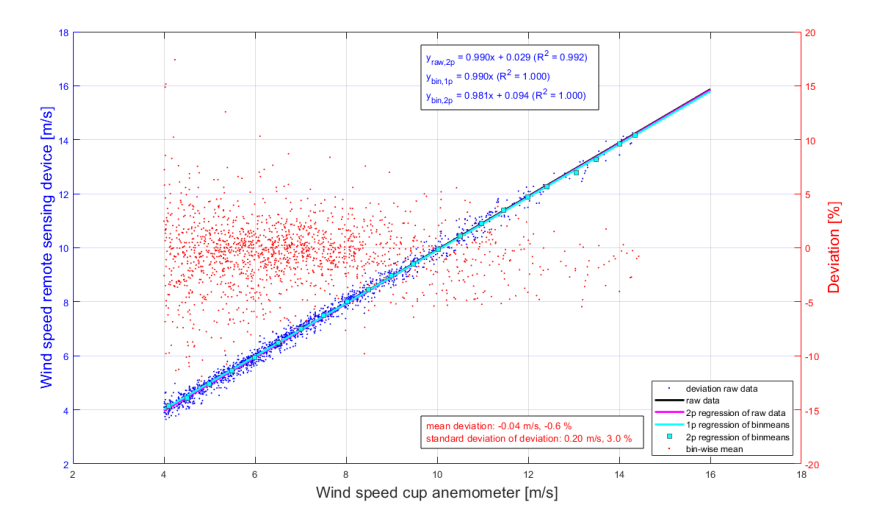


Figure 12: Wind speed comparison @44 m

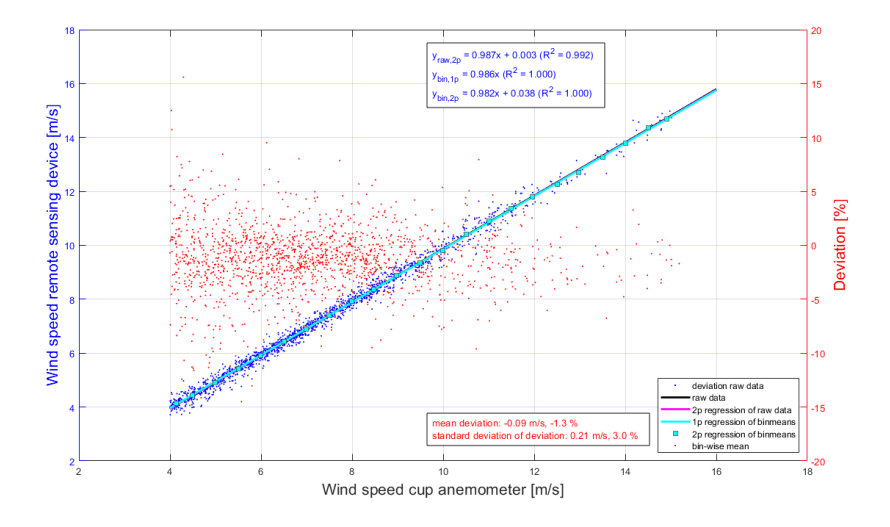


Figure 13: Wind speed comparison $@59\,\mathrm{m}$

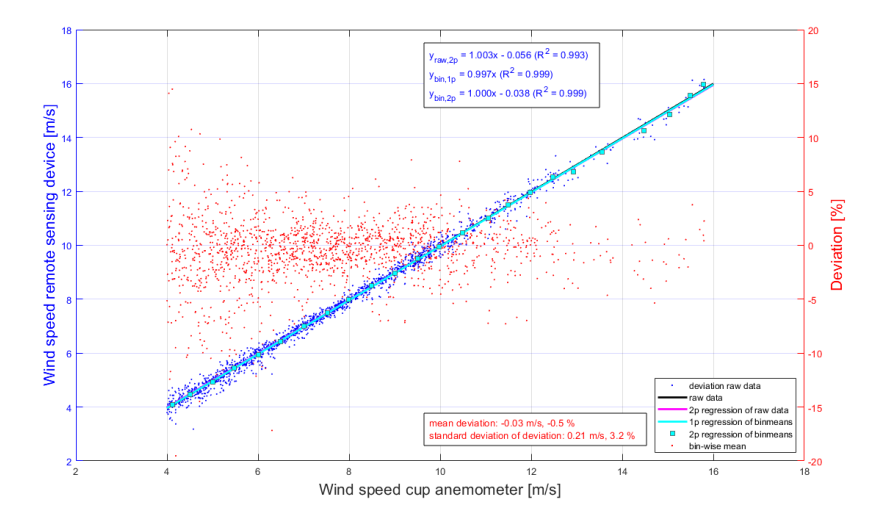


Figure 14: Wind speed comparison @90 m

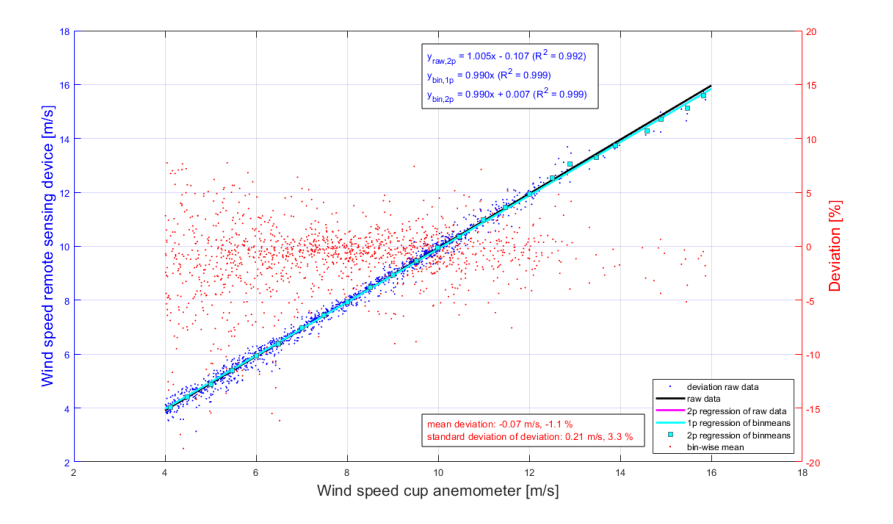


Figure 15: Wind speed comparison @100 m

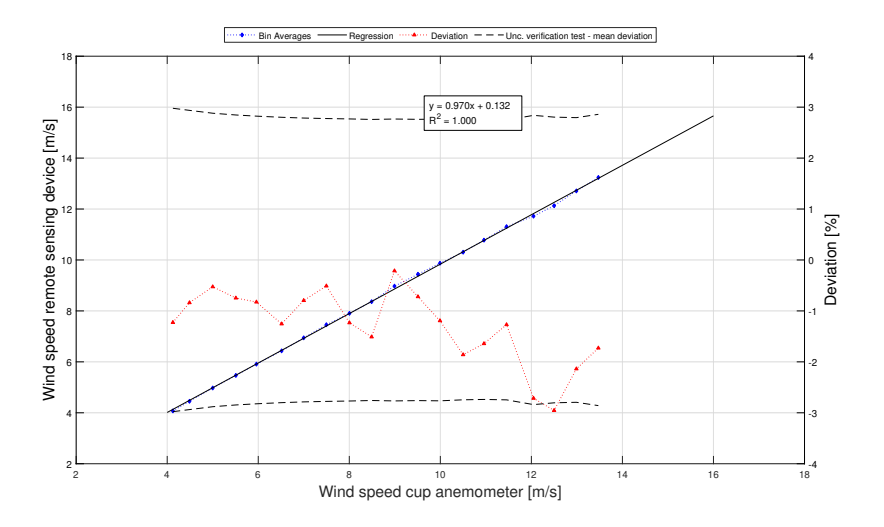


Figure 16: Bin-wise wind speed comparison @29 \mbox{m}

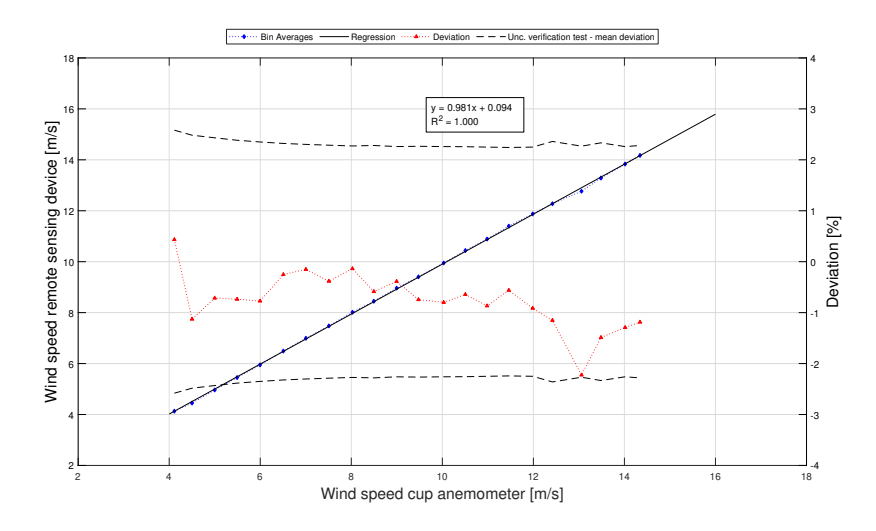


Figure 17: Bin-wise wind speed comparison @44 m

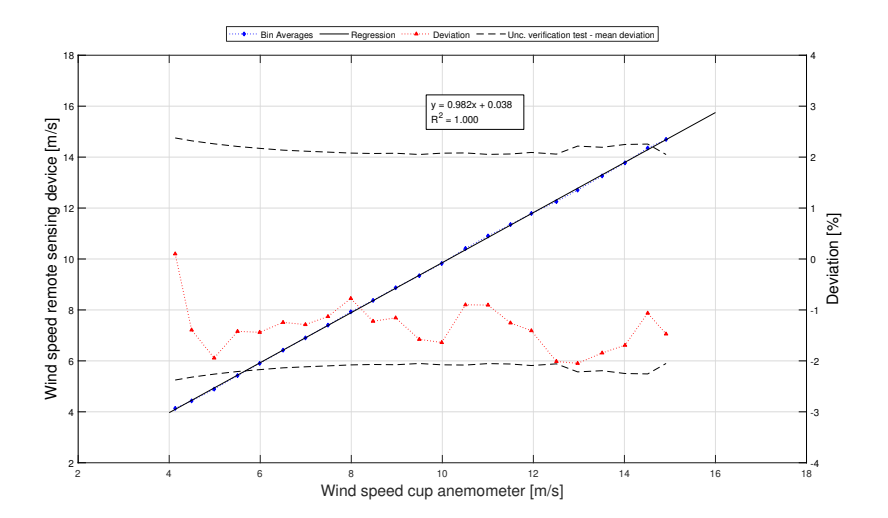


Figure 18: Bin-wise wind speed comparison $@59\,\mathrm{m}$

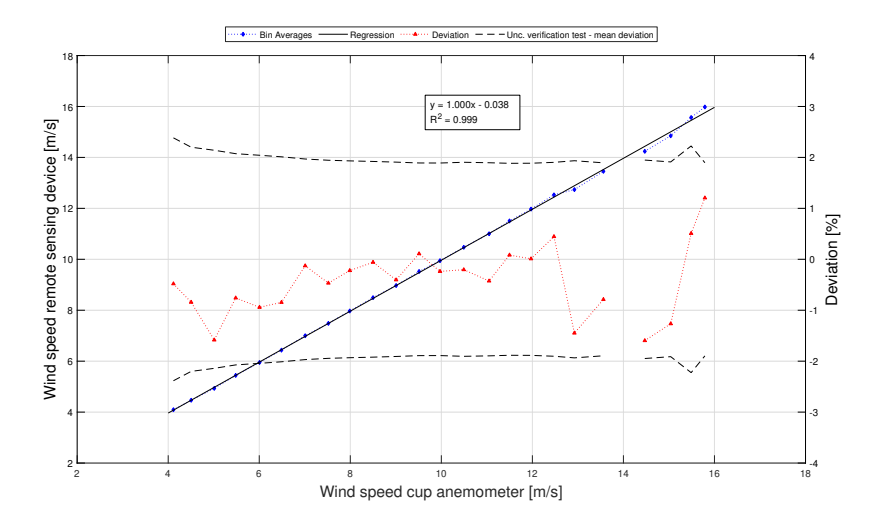


Figure 19: Bin-wise wind speed comparison @90 \mbox{m}

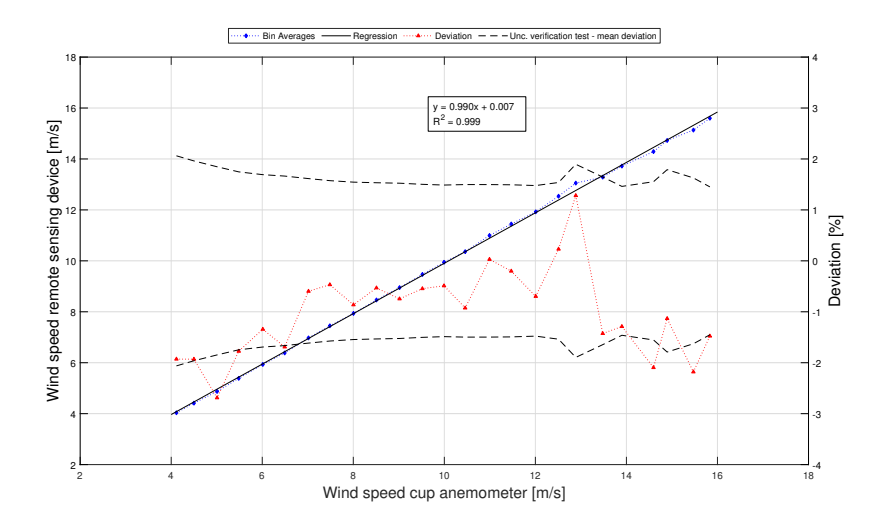


Figure 20: Bin-wise wind speed comparison $@100\,\mathrm{m}$

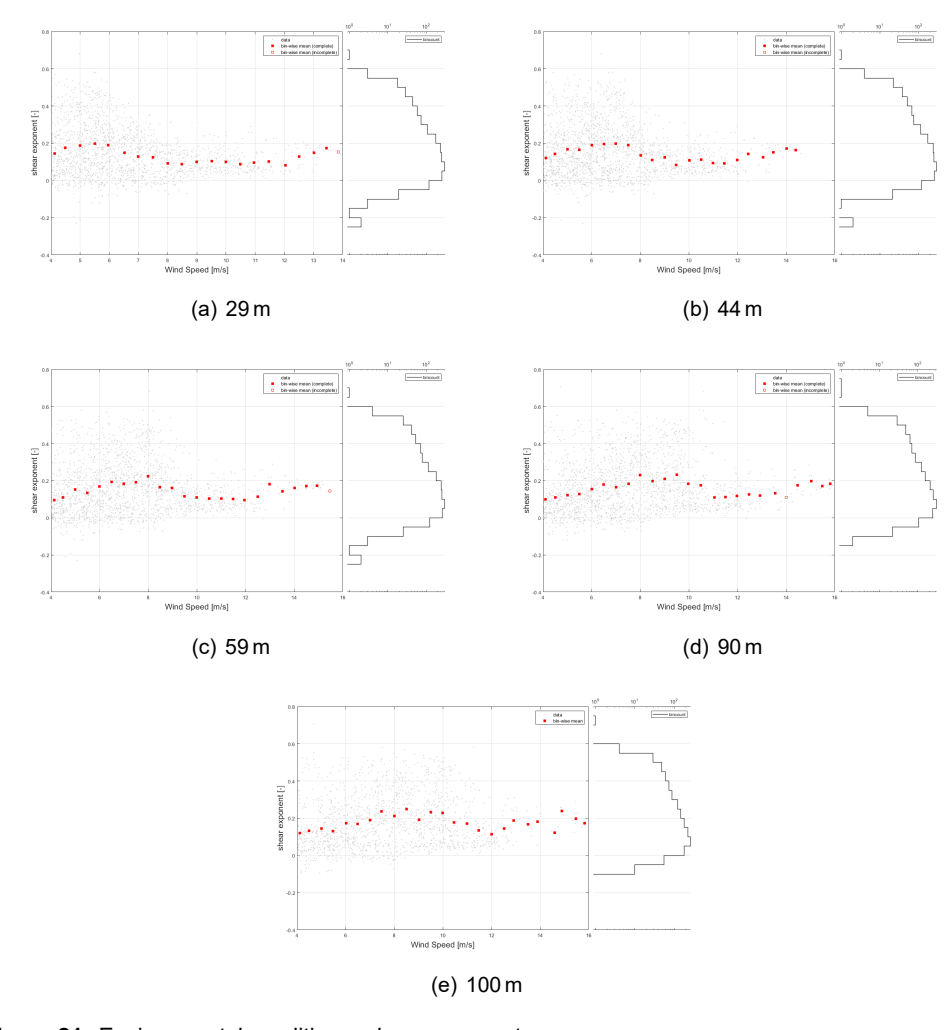


Figure 21: Environmental conditions: shear exponent

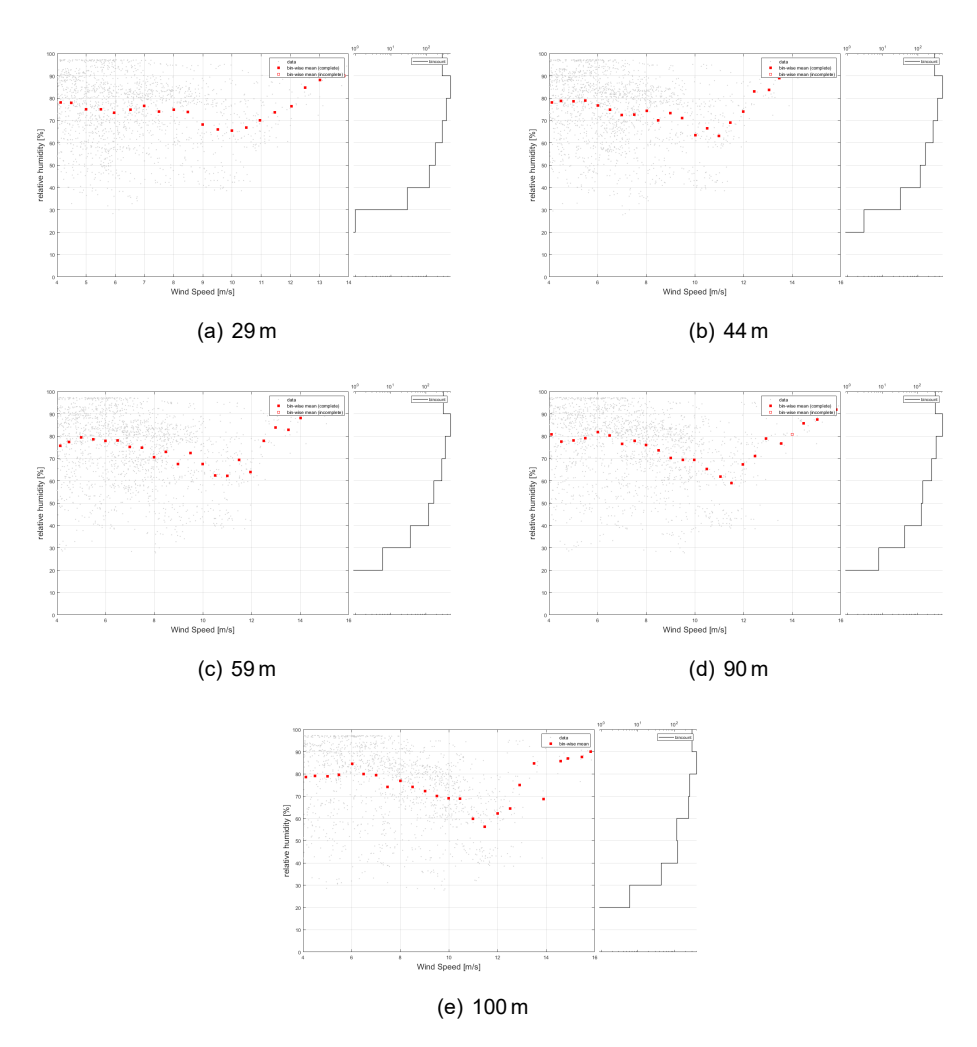


Figure 22: Environmental conditions: relative humidity

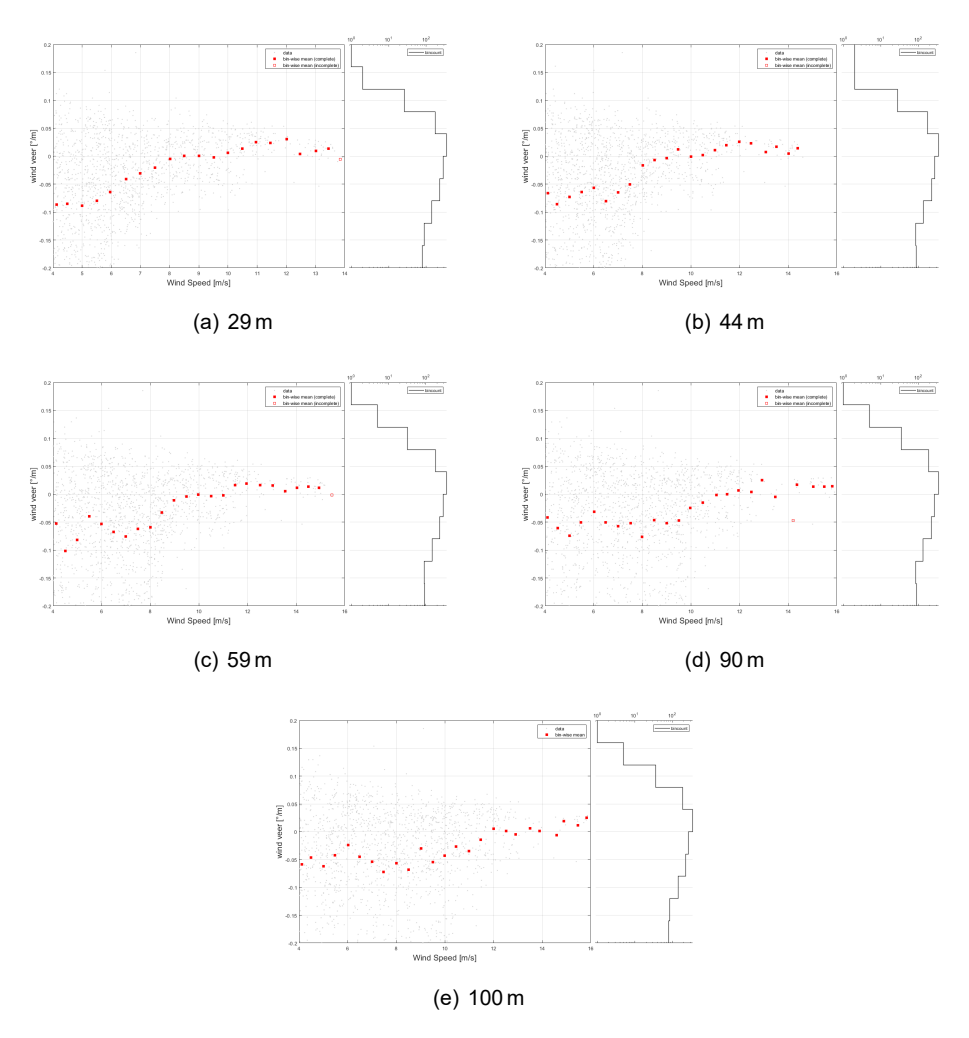


Figure 23: Environmental conditions: wind veer

Table 4: Uncertainty calculations arising from performance verification of the rsd @29 m in terms of systematic uncertainties.

V_{cup}	$V_{\sf rsd}$	data sets	V_{rsd} max	V_{rsd} min	V_{rsd} std	$V_{\mathrm{rsd}} rac{\mathrm{std}}{\sqrt{n}}$	mean deviation	V_{cup} uncertainty	mounting unc. rsd	separation unc.	$V_{\sf rsd}$ uncertainty
m/s	m/s	#	m/s	m/s	m/s	m/s	%	%	%	%	%
4.12	4.07	85	4.49	3.63	0.175	0.019	-1.227	2.070	0.10	2.07	3.221
4.49	4.45	165	5.45	3.61	0.256	0.020	-0.839	2.014	0.10	2.07	3.055
5.00	4.97	194	5.57	4.41	0.236	0.017	-0.526	1.953	0.10	2.07	2.928
5.51	5.47	208	6.13	4.64	0.252	0.017	-0.747	1.905	0.10	2.07	2.943
5.96	5.91	166	6.50	5.22	0.244	0.019	-0.826	1.871	0.10	2.07	2.942
6.51	6.43	139	7.22	5.65	0.244	0.021	-1.255	1.837	0.10	2.07	3.070
7.00	6.94	121	7.85	6.41	0.250	0.023	-0.796	1.812	0.10	2.07	2.898
7.50	7.46	88	8.39	6.92	0.251	0.027	-0.510	1.791	0.10	2.07	2.823
8.00	7.91	84	8.43	7.00	0.285	0.031	-1.233	1.773	0.10	2.07	3.031
8.49	8.36	64	9.16	7.69	0.262	0.033	-1.511	1.758	0.10	2.07	3.145
8.99	8.97	59	9.92	8.35	0.339	0.044	-0.213	1.745	0.10	2.07	2.775
9.51	9.44	51	10.17	8.76	0.338	0.047	-0.721	1.733	0.10	2.07	2.853
9.99	9.87	41	10.57	9.17	0.354	0.055	-1.193	1.723	0.10	2.07	3.012
10.50	10.31	34	10.95	9.74	0.292	0.050	-1.860	1.714	0.10	2.07	3.316
10.96	10.78	34	11.32	10.01	0.294	0.050	-1.643	1.707	0.10	2.07	3.193
11.45	11.31	18	11.69	10.88	0.258	0.061	-1.270	1.699	0.10	2.07	3.026
12.05	11.72	9	12.08	11.09	0.329	0.110	-2.715	1.692	0.10	2.07	3.928
12.50	12.13	9	12.56	11.49	0.302	0.101	-2.955	1.687	0.10	2.07	4.074
12.99	12.71	12	13.41	11.99	0.350	0.101	-2.138	1.682	0.10	2.07	3.518
13.47	13.24	8	13.69	12.45	0.379	0.134	-1.729	1.677	0.10	2.07	3.341
		0									
		0									
		0									
		0									
		0									

Table 5: Uncertainty calculations arising from performance verification of the rsd @44 m in terms of systematic uncertainties.

V_{cup}	V_{rsd}	data sets	V_{rsd} max	V_{rsd} min	V_{rsd} std	$V_{\mathrm{rsd}} rac{\mathrm{std}}{\sqrt{n}}$	mean deviation	$V_{ m cup}$ uncertainty	mounting unc. rsd	separation unc.	$V_{ m rsd}$ uncertainty
m/s	m/s	#	m/s	m/s	m/s	m/s	%	%	%	%	%
4.11	4.13	69	4.98	3.65	0.224	0.027	0.434	2.072	0.10	1.37	2.618
4.50	4.45	154	5.09	3.78	0.232	0.019	-1.128	2.013	0.10	1.37	2.727
5.00	4.96	147	5.51	4.22	0.241	0.020	-0.715	1.953	0.10	1.37	2.535
5.49	5.45	173	6.08	4.80	0.234	0.018	-0.737	1.906	0.10	1.37	2.495
6.00	5.95	162	6.74	5.38	0.229	0.018	-0.773	1.868	0.10	1.37	2.474
6.51	6.49	173	7.32	5.89	0.229	0.017	-0.253	1.837	0.10	1.37	2.335
7.00	6.99	139	7.61	6.30	0.228	0.019	-0.151	1.812	0.10	1.37	2.308
7.51	7.48	120	8.29	6.84	0.232	0.021	-0.384	1.791	0.10	1.37	2.319
8.02	8.01	103	8.60	7.38	0.227	0.022	-0.136	1.772	0.10	1.37	2.276
8.50	8.45	69	9.07	7.58	0.290	0.035	-0.586	1.758	0.10	1.37	2.355
9.00	8.96	56	9.58	8.53	0.235	0.031	-0.388	1.745	0.10	1.37	2.293
9.48	9.40	49	10.20	8.84	0.284	0.041	-0.745	1.734	0.10	1.37	2.385
10.03	9.95	42	10.61	9.39	0.289	0.045	-0.799	1.722	0.10	1.37	2.397
10.51	10.44	41	11.17	9.89	0.312	0.049	-0.644	1.714	0.10	1.37	2.347
10.98	10.89	41	11.34	10.30	0.320	0.050	-0.868	1.706	0.10	1.37	2.411
11.46	11.40	25	11.82	10.82	0.254	0.051	-0.561	1.699	0.10	1.37	2.311
11.99	11.88	17	12.27	11.48	0.249	0.060	-0.914	1.693	0.10	1.37	2.428
12.42	12.28	7	12.76	11.97	0.290	0.110	-1.152	1.688	0.10	1.37	2.627
13.06	12.77	10	13.22	12.46	0.253	0.080	-2.225	1.681	0.10	1.37	3.177
13.49	13.28	9	13.95	12.85	0.336	0.112	-1.488	1.677	0.10	1.37	2.768
14.01	13.83	8	14.13	13.44	0.240	0.085	-1.293	1.672	0.10	1.37	2.603
14.34	14.17	4	14.32	13.88	0.198	0.099	-1.187	1.670	0.10	1.37	2.572
		0									
		0									
		0									

Table 6: Uncertainty calculations arising from performance verification of the rsd @59 m in terms of systematic uncertainties.

V_{cup}	V_{rsd}	data sets	V_{rsd} max	V_{rsd} min	V_{rsd} std	$V_{rsd} frac{std}{\sqrt{n}}$	mean deviation	V_{cup} uncertainty	mounting unc. rsd	separation unc.	$V_{\sf rsd}$ uncertainty
m/s	m/s	#	m/s	m/s	m/s	m/s	%	%	%	%	%
4.13	4.14	68	4.56	3.71	0.171	0.021	0.101	2.069	0.10	1.02	2.378
4.49	4.43	130	5.06	3.73	0.236	0.021	-1.394	2.014	0.10	1.02	2.706
4.99	4.89	144	5.59	4.23	0.251	0.021	-1.944	1.954	0.10	1.02	2.981
5.50	5.42	135	5.95	4.64	0.234	0.020	-1.421	1.905	0.10	1.02	2.626
5.99	5.90	141	6.71	5.04	0.237	0.020	-1.439	1.869	0.10	1.02	2.606
6.50	6.42	155	6.97	5.89	0.221	0.018	-1.244	1.837	0.10	1.02	2.473
6.99	6.90	149	7.56	6.31	0.240	0.020	-1.288	1.813	0.10	1.02	2.477
7.49	7.40	125	8.34	6.64	0.234	0.021	-1.130	1.792	0.10	1.02	2.383
7.99	7.93	129	8.61	7.27	0.228	0.020	-0.775	1.774	0.10	1.02	2.219
8.48	8.37	118	9.03	7.64	0.263	0.024	-1.222	1.758	0.10	1.02	2.405
8.97	8.87	70	9.40	8.17	0.289	0.035	-1.155	1.745	0.10	1.02	2.376
9.49	9.34	64	9.83	8.74	0.228	0.029	-1.577	1.733	0.10	1.02	2.588
9.99	9.82	45	10.52	9.12	0.322	0.048	-1.639	1.723	0.10	1.02	2.646
10.51	10.41	39	11.11	9.70	0.349	0.056	-0.899	1.714	0.10	1.02	2.268
11.00	10.90	47	11.64	10.02	0.330	0.048	-0.904	1.706	0.10	1.02	2.244
11.50	11.35	32	11.99	10.58	0.325	0.057	-1.255	1.699	0.10	1.02	2.414
11.96	11.79	17	12.26	11.24	0.309	0.075	-1.407	1.693	0.10	1.02	2.521
12.51	12.25	16	12.68	11.54	0.264	0.066	-2.012	1.687	0.10	1.02	2.878
12.97	12.71	5	13.14	12.40	0.285	0.128	-2.048	1.682	0.10	1.02	3.018
13.51	13.26	6	13.51	12.67	0.311	0.127	-1.844	1.677	0.10	1.02	2.865
14.01	13.78	9	14.64	13.30	0.449	0.150	-1.693	1.672	0.10	1.02	2.815
14.51	14.36	5	14.76	13.90	0.354	0.158	-1.063	1.668	0.10	1.02	2.494
14.91	14.70	9	14.98	14.27	0.252	0.084	-1.472	1.665	0.10	1.02	2.525
		0									
		0									

Table 7: Uncertainty calculations arising from performance verification of the rsd @90 m in terms of systematic uncertainties.

V_{cup}	$V_{\sf rsd}$	data sets	$V_{\sf rsd}$ max	$V_{\sf rsd}$ min	$V_{\sf rsd}$ std	$V_{rsd} \frac{std}{\sqrt{n}}$	mean deviation	V_{cup} uncertainty	mounting unc. rsd	separation unc.	$V_{\sf rsd}$ uncertainty
V cup	Vrsd	uala sels	Vrsd IIIax	V rsd IIIIII	Vrsd Stu	$V \operatorname{rsd} \sqrt{n}$	mean deviation	V cup differ tallity	mounting unc. 1su	Separation unc.	V _{rsd} uncertainty
m/s	m/s	#	m/s	m/s	m/s	m/s	%	%	%	%	%
4.11	4.09	51	4.71	3.37	0.274	0.038	-0.481	2.072	0.10	0.67	2.432
4.50	4.47	122	5.21	3.18	0.258	0.023	-0.843	2.012	0.10	0.67	2.357
5.01	4.93	119	5.67	4.14	0.274	0.025	-1.584	1.951	0.10	0.67	2.663
5.48	5.44	144	6.09	4.82	0.245	0.020	-0.759	1.907	0.10	0.67	2.208
6.01	5.95	118	6.45	5.23	0.261	0.024	-0.943	1.868	0.10	0.67	2.249
6.49	6.43	106	7.01	5.22	0.255	0.025	-0.845	1.838	0.10	0.67	2.182
7.01	7.00	142	7.46	6.30	0.222	0.019	-0.127	1.812	0.10	0.67	1.973
7.52	7.48	116	7.87	7.08	0.183	0.017	-0.467	1.790	0.10	0.67	2.000
7.99	7.97	105	8.50	7.48	0.207	0.020	-0.222	1.774	0.10	0.67	1.945
8.50	8.49	104	9.13	7.93	0.240	0.024	-0.059	1.758	0.10	0.67	1.922
9.01	8.97	103	9.55	8.24	0.245	0.024	-0.404	1.744	0.10	0.67	1.950
9.51	9.52	107	10.11	9.07	0.220	0.021	0.109	1.733	0.10	0.67	1.894
9.97	9.95	80	10.51	9.38	0.250	0.028	-0.238	1.723	0.10	0.67	1.905
10.49	10.47	56	11.24	9.73	0.320	0.043	-0.204	1.714	0.10	0.67	1.916
11.05	11.00	38	11.59	10.25	0.274	0.044	-0.426	1.705	0.10	0.67	1.943
11.50	11.51	40	11.97	10.61	0.273	0.043	0.083	1.699	0.10	0.67	1.886
11.97	11.97	35	12.46	11.07	0.290	0.049	0.009	1.693	0.10	0.67	1.886
12.47	12.53	20	13.32	12.02	0.281	0.063	0.446	1.687	0.10	0.67	1.955
12.92	12.74	9	13.10	12.41	0.242	0.081	-1.448	1.682	0.10	0.67	2.417
13.56	13.45	10	13.76	13.04	0.216	0.068	-0.789	1.676	0.10	0.67	2.052
		2	14.22	13.63							
14.47	14.24	10	14.70	13.92	0.319	0.101	-1.597	1.669	0.10	0.67	2.518
15.04	14.85	7	15.11	14.47	0.239	0.090	-1.266	1.664	0.10	0.67	2.292
15.49	15.57	5	16.12	15.13	0.447	0.200	0.508	1.661	0.10	0.67	2.282
15.79	15.98	3	16.15	15.86	0.154	0.089	1.205	1.659	0.10	0.67	2.246

Table 8: Uncertainty calculations arising from performance verification of the rsd @100 m in terms of systematic uncertainties.

I.	V	data sets	V mov	V min	V etd	v std	moon deviation	V upcortainty	mounting upo rad	congration upo	$V_{ m rsd}$ uncertainty
V_{cup}	V_{rsd}	uala sels	$V_{\sf rsd}$ max	$V_{\sf rsd}$ min	$V_{\sf rsd}$ std	$V_{\mathrm{rsd}} \frac{\mathrm{std}}{\sqrt{n}}$	mean deviation	$V_{\sf cup}$ uncertainty	mounting unc. rsd	separation unc.	V _{rsd} uncertainty
m/s	m/s	#	m/s	m/s	m/s	m/s	%	%	%	%	%
4.11	4.03	43	4.51	3.54	0.237	0.036	-1.929	1.744	0.10	0.60	2.824
4.50	4.41	81	4.89	3.13	0.315	0.035	-1.931	1.674	0.10	0.60	2.752
5.01	4.87	82	5.39	4.09	0.291	0.032	-2.689	1.600	0.10	0.60	3.262
5.48	5.39	115	5.94	4.62	0.279	0.026	-1.774	1.545	0.10	0.60	2.490
6.01	5.93	87	6.33	5.36	0.243	0.026	-1.343	1.495	0.10	0.60	2.160
6.49	6.38	92	6.94	5.37	0.280	0.029	-1.691	1.459	0.10	0.60	2.372
7.02	6.97	87	7.54	6.40	0.242	0.026	-0.597	1.425	0.10	0.60	1.722
7.48	7.45	94	7.90	6.76	0.205	0.021	-0.468	1.400	0.10	0.60	1.642
8.00	7.93	96	8.46	7.41	0.183	0.019	-0.864	1.376	0.10	0.60	1.770
8.51	8.46	87	8.86	7.93	0.214	0.023	-0.532	1.356	0.10	0.60	1.623
9.02	8.95	79	9.41	8.23	0.243	0.027	-0.747	1.339	0.10	0.60	1.697
9.52	9.47	97	10.18	8.67	0.240	0.024	-0.546	1.324	0.10	0.60	1.598
9.99	9.94	96	10.48	9.34	0.232	0.024	-0.490	1.311	0.10	0.60	1.567
10.46	10.36	66	11.17	9.79	0.286	0.035	-0.926	1.300	0.10	0.60	1.760
10.99	10.99	39	11.73	10.52	0.258	0.041	0.029	1.289	0.10	0.60	1.497
11.47	11.45	49	12.12	10.56	0.314	0.045	-0.202	1.280	0.10	0.60	1.507
12.01	11.92	34	12.55	11.36	0.255	0.044	-0.697	1.270	0.10	0.60	1.634
12.51	12.54	16	13.26	12.18	0.288	0.072	0.230	1.263	0.10	0.60	1.555
12.89	13.05	7	13.69	12.39	0.428	0.162	1.282	1.257	0.10	0.60	2.288
13.48	13.29	5	13.56	12.87	0.254	0.113	-1.427	1.250	0.10	0.60	2.178
13.90	13.72	3	13.80	13.62	0.092	0.053	-1.290	1.245	0.10	0.60	1.949
14.59	14.29	3	14.47	14.13	0.168	0.097	-2.096	1.237	0.10	0.60	2.609
14.89	14.73	4	14.98	14.24	0.332	0.166	-1.133	1.234	0.10	0.60	2.119
15.47	15.13	6	15.54	14.66	0.317	0.130	-2.181	1.229	0.10	0.60	2.721
15.83	15.60	4	15.75	15.44	0.129	0.065	-1.477	1.226	0.10	0.60	2.071

 Table 9: Environmental conditions experienced during verification test for LiDAR measurements @29 m.

wind speed	shear exponent	turbulence intensity	precipitation	wind direction	air temperature	relative humidity	air density	flow inclination	wind veer
m/s		%	%	٥	°C	%	kg/m³	٥	°/m
4.125	0.1203	11.28	5.92	130.8	14.37	78.19	1.211	2.071	-0.0661
4.500	0.1426	10.80	10.53	144.1	14.19	78.87	1.210	2.381	-0.0862
5.000	0.1678	10.51	14.95	141.7	13.43	78.60	1.214	2.367	-0.0728
5.500	0.1643	9.82	10.39	147.2	13.44	78.99	1.214	1.755	-0.0642
6.000	0.1893	9.18	13.99	144.1	13.61	76.67	1.214	1.522	-0.0564
6.500	0.1964	8.77	8.30	124.3	13.94	74.91	1.212	1.488	-0.0804
7.000	0.1971	9.29	13.02	123.7	13.66	72.57	1.212	1.468	-0.0647
7.500	0.1888	9.25	12.27	98.6	15.09	72.70	1.206	1.218	-0.0502
8.000	0.1344	9.91	7.02	122.0	13.80	74.28	1.209	1.239	-0.0167
8.500	0.1102	10.41	11.67	141.7	13.60	70.08	1.212	1.158	-0.0068
9.000	0.1250	11.20	18.44	165.9	11.56	73.36	1.219	1.399	-0.0033
9.500	0.0838	10.83	0.65	181.2	11.61	71.14	1.222	1.070	0.0120
10.000	0.1079	11.85	3.59	198.5	11.05	63.50	1.223	1.389	-0.0009
10.500	0.1115	12.21	13.19	199.1	10.69	66.47	1.224	1.352	0.0022
11.000	0.0944	11.59	4.44	222.4	10.32	63.06	1.226	1.370	0.0106
11.500	0.0922	10.86	11.54	200.7	9.97	69.11	1.230	0.587	0.0197
12.000	0.1093	11.74	11.76	159.7	10.10	74.09	1.228	0.637	0.0260
12.500	0.1437	12.65	15.00	120.6	11.62	83.01	1.219	0.600	0.0230
13.000	0.1234	11.35	10.00	147.8	10.44	83.73	1.224	0.423	0.0077
13.500	0.1501	11.68	34.00	195.4	10.50	88.97	1.219	0.522	0.0169
14.000	0.1717	10.87	58.79	213.7	10.19	89.84	1.216	0.598	0.0049
14.500	0.1641	11.03	78.00	191.9	10.08	91.54	1.218	0.452	0.0141
15.000									
15.500									
15.875									

 Table 10:
 Environmental conditions experienced during verification test for LiDAR measurements @44 m.

wind speed	shear exponent	turbulence intensity	precipitation	wind direction	air temperature	relative humidity	air density	flow inclination	wind veer
m/s		%	%	٥	°C	%	kg/m³	٥	°/m
4.125	0.1203	11.28	5.92	130.8	14.37	78.19	1.211	2.071	-0.0661
4.500	0.1426	10.80	10.53	144.1	14.19	78.87	1.210	2.381	-0.0862
5.000	0.1678	10.51	14.95	141.7	13.43	78.60	1.214	2.367	-0.0728
5.500	0.1643	9.82	10.39	147.2	13.44	78.99	1.214	1.755	-0.0642
6.000	0.1893	9.18	13.99	144.1	13.61	76.67	1.214	1.522	-0.0564
6.500	0.1964	8.77	8.30	124.3	13.94	74.91	1.212	1.488	-0.0804
7.000	0.1971	9.29	13.02	123.7	13.66	72.57	1.212	1.468	-0.0647
7.500	0.1888	9.25	12.27	98.6	15.09	72.70	1.206	1.218	-0.0502
8.000	0.1344	9.91	7.02	122.0	13.80	74.28	1.209	1.239	-0.0167
8.500	0.1102	10.41	11.67	141.7	13.60	70.08	1.212	1.158	-0.0068
9.000	0.1250	11.20	18.44	165.9	11.56	73.36	1.219	1.399	-0.0033
9.500	0.0838	10.83	0.65	181.2	11.61	71.14	1.222	1.070	0.0120
10.000	0.1079	11.85	3.59	198.5	11.05	63.50	1.223	1.389	-0.0009
10.500	0.1115	12.21	13.19	199.1	10.69	66.47	1.224	1.352	0.0022
11.000	0.0944	11.59	4.44	222.4	10.32	63.06	1.226	1.370	0.0106
11.500	0.0922	10.86	11.54	200.7	9.97	69.11	1.230	0.587	0.0197
12.000	0.1093	11.74	11.76	159.7	10.10	74.09	1.228	0.637	0.0260
12.500	0.1437	12.65	15.00	120.6	11.62	83.01	1.219	0.600	0.0230
13.000	0.1234	11.35	10.00	147.8	10.44	83.73	1.224	0.423	0.0077
13.500	0.1501	11.68	34.00	195.4	10.50	88.97	1.219	0.522	0.0169
14.000	0.1717	10.87	58.79	213.7	10.19	89.84	1.216	0.598	0.0049
14.500	0.1641	11.03	78.00	191.9	10.08	91.54	1.218	0.452	0.0141
15.000									
15.500									
15.875									

 Table 11: Environmental conditions experienced during verification test for LiDAR measurements @59 m.

wind speed	shear exponent	turbulence intensity	precipitation	wind direction	air temperature	relative humidity	air density	flow inclination	wind veer
m/s		%	%	٥	°C	%	kg/m³	۰	°/m
4.125	0.0961	12.75	9.03	142.7	14.51	75.71	1.209	2.005	-0.0524
4.500	0.1107	10.96	9.97	134.2	14.67	77.42	1.208	2.215	-0.1015
5.000	0.1535	10.40	13.07	138.6	14.13	79.40	1.211	2.400	-0.0818
5.500	0.1350	10.64	11.52	144.2	13.88	78.61	1.213	1.880	-0.0396
6.000	0.1697	9.45	14.60	150.3	13.74	77.91	1.213	1.650	-0.0534
6.500	0.1935	9.10	10.04	139.3	13.51	78.13	1.214	1.631	-0.0673
7.000	0.1845	8.84	11.93	116.5	14.21	75.29	1.210	1.436	-0.0757
7.500	0.1914	9.09	12.37	112.2	13.65	74.96	1.212	1.314	-0.0623
8.000	0.2240	8.68	10.80	119.5	14.07	70.53	1.210	1.307	-0.0595
8.500	0.1646	9.47	7.82	123.1	13.76	73.00	1.210	1.197	-0.0329
9.000	0.1601	9.85	11.38	156.6	13.49	67.57	1.214	1.342	-0.0110
9.500	0.1164	10.44	10.10	179.5	11.45	72.53	1.219	1.448	-0.0038
10.000	0.1107	10.81	6.43	171.7	11.92	67.59	1.221	1.185	-0.0004
10.500	0.1036	11.74	3.95	202.7	11.18	62.40	1.222	1.192	-0.0033
11.000	0.1043	11.49	11.12	189.8	11.56	62.19	1.221	1.315	-0.0019
11.500	0.1017	11.40	11.93	227.6	9.77	69.41	1.228	1.430	0.0161
12.000	0.0959	9.43	14.92	241.1	9.68	63.96	1.230	0.472	0.0188
12.500	0.1141	11.54	27.78	136.9	10.35	77.85	1.225	0.527	0.0162
13.000	0.1819	12.06	24.69	119.0	11.02	83.96	1.221	0.377	0.0158
13.500	0.1434	12.07	10.27	172.9	9.77	82.92	1.222	0.601	0.0058
14.000	0.1617	11.87	39.86	214.2	10.32	88.14	1.217	0.693	0.0113
14.500	0.1721	11.11	48.64	201.4	10.10	90.96	1.217	0.688	0.0139
15.000	0.1732	11.08	70.45	190.1	10.06	91.06	1.217	0.482	0.0113
15.500									
15.875									

wind speed	shear exponent	turbulence intensity	precipitation	wind direction	air temperature	relative humidity	air density	flow inclination	wind veer
m/s		%	%	0	°C	%	kg/m³	0	°/m
4.125	0.1001	11.85	16.74	153.6	14.31	80.82	1.210	2.612	-0.0415
4.500	0.1105	11.11	9.50	138.7	14.75	77.51	1.208	2.170	-0.0604
5.000	0.1219	10.05	12.90	130.9	14.28	78.18	1.210	2.404	-0.0743
5.500	0.1281	9.46	9.00	133.5	14.78	79.14	1.208	1.840	-0.0506
6.000	0.1541	9.03	16.88	144.1	13.75	81.88	1.213	1.674	-0.0310
6.500	0.1789	8.40	13.61	146.6	13.18	80.27	1.215	1.769	-0.0507
7.000	0.1642	7.89	14.75	130.6	14.11	76.63	1.212	1.547	-0.0569
7.500	0.1839	7.55	8.78	109.9	13.57	77.91	1.213	1.228	-0.0518
8.000	0.2303	7.08	10.95	126.2	13.18	76.00	1.214	1.245	-0.0760
8.500	0.1989	8.04	8.79	148.0	12.57	73.76	1.216	1.463	-0.0464
9.000	0.2100	7.94	16.56	163.0	11.77	70.30	1.219	1.374	-0.0518
9.500	0.2333	7.60	6.93	170.6	11.97	69.43	1.219	1.505	-0.0471
10.000	0.1846	8.23	3.91	157.4	11.96	69.40	1.219	1.270	-0.0247
10.500	0.1747	9.17	8.33	166.2	12.88	65.26	1.217	1.283	-0.0153
11.000	0.1092	9.21	4.03	203.0	11.75	61.93	1.221	1.020	-0.0011
11.500	0.1119	10.51	7.38	200.3	11.07	59.06	1.224	1.567	0.0001
12.000	0.1184	10.09	12.06	191.0	10.31	67.35	1.228	0.988	0.0066
12.500	0.1260	10.15	15.00	168.2	10.94	71.18	1.224	1.386	0.0038
13.000	0.1211	10.97	18.81	111.1	11.16	78.91	1.226	0.318	0.0251
13.500	0.1322	10.01	20.00	102.8	11.58	76.71	1.222	0.466	-0.0046
14.000									
14.500	0.1747	11.27	14.81	147.6	10.64	85.70	1.222	0.649	0.0174
15.000	0.1974	10.18	33.80	231.9	10.48	87.51	1.215	0.959	0.0137
15.500	0.1712	9.18	24.37	240.0	10.36	91.42	1.216	0.754	0.0138
15.875	0.1840	9.53	83.63	192.0	10.05	91.90	1.218	0.608	0.0145

 Table 13: Environmental conditions experienced during verification test for LiDAR measurements @100 m.

wind speed	shear exponent	turbulence intensity	precipitation	wind direction	air temperature	relative humidity	air density	flow inclination	wind veer
m/s		%	%	٥	°C	%	kg/m³	۰	°/m
4.125	0.1196	11.68	15.79	177.3	15.00	78.56	1.206	2.896	-0.0584
4.500	0.1321	11.46	12.29	179.5	14.52	79.19	1.208	2.381	-0.0464
5.000	0.1450	9.92	16.14	167.3	13.77	79.03	1.213	2.401	-0.0618
5.500	0.1295	10.09	12.59	174.7	14.12	79.66	1.211	2.105	-0.0420
6.000	0.1738	8.81	19.54	179.1	13.51	84.56	1.214	1.987	-0.0241
6.500	0.1702	8.18	16.72	163.7	13.44	80.07	1.214	1.737	-0.0450
7.000	0.1905	7.85	19.88	169.6	12.99	79.54	1.216	1.640	-0.0535
7.500	0.2362	7.22	13.98	150.2	12.62	74.18	1.218	1.523	-0.0721
8.000	0.2133	7.32	12.96	135.1	13.07	76.95	1.214	1.376	-0.0564
8.500	0.2493	7.52	8.68	171.6	11.39	74.22	1.221	1.618	-0.0682
9.000	0.1911	8.25	16.55	184.1	11.82	72.36	1.218	1.518	-0.0299
9.500	0.2328	7.79	11.41	193.3	10.90	70.04	1.222	1.654	-0.0546
10.000	0.2281	7.18	4.53	163.6	11.89	69.13	1.219	1.332	-0.0430
10.500	0.1778	8.74	4.94	172.7	11.62	68.88	1.221	1.397	-0.0262
11.000	0.1707	8.69	8.23	183.3	13.44	59.84	1.214	1.278	-0.0347
11.500	0.1351	9.98	2.57	205.1	12.10	56.32	1.219	1.500	-0.0141
12.000	0.1151	9.58	8.67	225.8	10.48	62.27	1.226	1.165	0.0056
12.500	0.1450	9.75	30.86	217.2	11.23	64.46	1.221	1.350	0.0015
13.000	0.1881	9.59	50.00	207.8	11.67	74.96	1.217	2.339	-0.0046
13.500	0.1673	11.35	70.10	231.6	8.68	84.76	1.222	1.512	0.0059
14.000	0.1807	6.55	33.33	197.8	13.27	68.71	1.213	0.467	0.0012
14.500	0.1229	9.91	0.00	244.0	9.12	85.83	1.219	0.670	-0.0060
15.000	0.2379	11.23	37.03	227.5	11.12	86.99	1.215	1.281	0.0188
15.500	0.1975	10.22	38.63	231.6	10.37	87.68	1.215	0.966	0.0115
15.875	0.1725	9.27	30.47	235.9	10.56	90.01	1.215	0.705	0.0253

6 Sensitivities

This chapter investigates the sensitivity of the LiDAR measurement for various environmental variables (EVs). The sensitivity analysis is performed in accordance with the classification analysis specified in annex L.2 [5]. However, for this analysis we use the same dataset as for the verification analysis. As a result the wind speed range is restricted to $4\,\mathrm{m/s}$ to $16\,\mathrm{m/s}$.

6.1 Sensitivity analysis

The basis of this analysis is the deviation between the wind speeds measured by the ref, v_{ref} , and the rsd, v_{rsd} . The deviation is defined in eq. (4.1). Subsequently the sensitivity of this deviation is tested against various EVs. The list of variables is based on table L.2 [5]. The variables considered are described below.

Unless stated otherwise the EVs are height-independent, meaning the same value was used for the sensitivity analysis at each comparison height.

1. Shear exponent [-]

The shear exponent, α , is computed by fitting a power law wind shear model through the $v_{\rm ref}$ measurements at 44 m, 59 m, 90 m and 100 m. The power law is defined by

$$\frac{v_{\text{ref}}}{v_r} = \left(\frac{h}{h_r}\right)^{\alpha} \tag{6.1}$$

2. Reference turbulence intensity [-]

The reference turbulence intensity, measured by MM4, is defined by

reference turbulence intensity =
$$\frac{\text{std}(v_{\text{ref}})}{\text{mean}(v_{\text{ref}})}$$
 (6.2)

This variable is height-dependent.

3. Precipitation [%]

The rain sensor returns a 0% to 100% signal indicating the amount of time precipitation was detected in the 10-minute interval. The precipitation is measured at $96\,\text{m}$.

4. Reference wind direction [°]

The wind direction, as measured by MM4, is height-dependent.

5. Air temperature [°C]

The air temperature is measured at 96 m.

6. Relative humidity [%RH]

The relative humidity is measured at 96 m. (The relative humidity was added to the list of EVs, because it used as in the MEASNET icing criterion in chapter 3.)

7. Air density [kg/m³]

The air density is computed from the air pressure, air temperature and relative humidity, all measured at 96 m in accordance with equation (12) of IEC 61400-12-1:2017.

8. Flow inclination [°]

The flow inclination is defined as

flow inclination =
$$\arctan\left(\frac{v_{\text{vert}}}{v_{\text{hor}}}\right)$$
 (6.3)

The horizontal (v_{hor}) and vertical (v_{vert}) wind speed components are measured by a sonic anemometer at a height of 87 m.

9. Wind veer [°/m]

The wind veer is computed as the difference between the wind direction measurements by MM4 at 42 m and 97 m, divided by the height difference. This definition was taken from IEC 61400-12-1:2017.

wind veer =
$$\frac{v_{d,42} - v_{d,97}}{97 - 42} \tag{6.4}$$

10. Reference wind speed [m/s]

This wind speed, as measured by MM4, is height-dependent.

The sensitivity analysis leads to the results presented in table 16, which is presented in the same format as table L.2 [5]. In this table column 'm' represents the slope of the two-parameter regression of the bin-wise averaged data. Column ' r^2 ' represents the correlation coefficient of the two-parameter regression of the scatter data.

For the computation of the bin-wise averages, only those bins are included that meet the following bin-count requirement, stipulated by the criterion in eq. (6.5) [5, eq. L.2]. When the reference wind speed is used as the EV, also the criterion in equation (L.3) needs to be applied.

$$n_i > \frac{N}{2 \cdot n_b} \tag{6.5}$$

The sensitivity, presented in column 'sens.', is defined by

sensitivity =
$$m \cdot \text{std}$$
 (6.6)

where 'std' is the standard deviation of the EV data.

The sensitivity of the LiDAR for an EV is considered as significant if either the sensitivity exceeds a value of 0.5, or the product of sensitivity and r exceeds 0.1. In table 16, the sensitivity criteria that exceed their threshold value are highlighted in red. The regressions associated with these significant sensitivities are presented in fig. 28. In case a significant sensitivity for an EV is observed for at least one comparison height, that EV must be considered as significant for all comparison heights. Table 14 provides an overview of the significant sensitivities.

6.2 Impact on accuracy

Although our interest is not in determining an accuracy class, but rather investigate the sensitivities presented in section 6.1, we would be amiss not to present the impact these sensitivities have on the accuracy.

The basis for the accuracy class is the product of m, as already presented in table 16, and the range of the EV. The EV ranges are largely prescribed by table L.3 [5]. The

flow inclination wind veer

reference wind speed

environmental variable comparison height overall 100 m 29 m 90 m 59 m 44 m shear exponent **√** \checkmark turbulence intensity precipitation wind direction air temperature relative humidity **√ √** air density

Table 14: Overview of significant sensitivities

results are presented in table 17, which is presented in a similar format as table L.6 [5]. Because precipitation has only a single bin (0%) that meets the bin count criterion, no sensitivity can be computed for this EV.

 \checkmark

The range is a defined quantity, presented in the column 'range' of table 17. The IEC 61400-12-1 standard defines the measured range of variation through the ratio of bins that meet the criterion in eq. (6.5). The result is presented in the column 'covered range'. The measured range of variation is considered sufficient if the covered range is at least 25 %.

For the relative humidity no range is prescribed; we used 0% to 100%. The prescribed flow inclination range of -3° to 3° was modified to -1° to 5° to better cover the measured range.

The EVs precipitation and air density do not meet the range requirement. For the precipitation this is caused by our choice of the metric: the amount of time precipitation is registered in a 10-minute interval. This causes most samples to fall in either the 0 % or the 100 % bin. For the air density this is caused by the limited variation of air density at the site with respect to the prescribed range.

The last column of table 17 represents the contribution to the preliminary accuracy class for each EV. From this we can draw the conclusion that shear and turbulence have the highest influence on the accuracy.

In order to obtain the preliminary accuracy class, these contributions have to be added in quadrature for each height. The results are presented in table 15, similar to table L.7 [5].

Table 15: Preliminary accuracy classes

height	considering all variables	considering only significant variables
m	-	
29	16.0	12.4
44	11.5	5.5
59	8.4	6.4
90	7.5	4.0
100	10.7	4.5

It should be noted that the results in table 15 cannot be used directly to derive the final accuracy class numbers, because the interdependency between the EVs has not been eliminated.

Table 16: Parameters derived from the sensitivity analysis of the rsd

height	variable	avg	std	m	sens.	r^2	sens. $ imes r$
m	-	unit	unit	1/unit			-
29 44 59 90 100	shear exponent	0.141 0.153 0.153 0.159 0.176	0.114 0.126 0.127 0.130 0.131	6.363 1.815 2.959 0.117 -1.682	0.726 0.228 0.375 0.015 -0.221	0.031 0.000 0.003 0.001 0.007	0.127 0.002 0.021 0.000 -0.019
29 44 59 90 100	turbulence intensity	11.214 9.646 9.496 8.488 8.318	2.358 2.462 2.423 2.536 2.629	-0.098 -0.033 -0.035 -0.008 0.029	-0.230 -0.081 -0.085 -0.021 0.076	0.003 0.000 0.000 0.000 0.001	-0.013 -0.002 -0.001 -0.000 0.002
29 44 59 90 100	precipitation	0.055 0.061 0.059 0.061 0.066	0.668 0.695 0.688 0.691 0.725			0.001 0.001 0.000 0.000 0.000	
29 44 59 90 100	wind direction	137.127 138.039 137.985 141.290 171.478	99.425 98.355 98.339 98.078 83.345	-0.001 -0.001 0.002 0.001 -0.003	-0.078 -0.125 0.166 0.101 -0.215	0.001 0.003 0.006 0.002 0.006	-0.002 -0.007 0.013 0.005 -0.017
29 44 59 90 100	air temperature	13.620 13.490 13.630 13.318 12.849	4.599 4.570 4.657 4.544 4.655	0.033 0.044 0.034 0.067 0.067	0.153 0.200 0.159 0.304 0.313	0.001 0.007 0.002 0.008 0.013	0.005 0.017 0.006 0.027 0.036
29 44 59 90 100	relative humidity	74.378 75.114 75.002 75.744 75.351	14.312 14.242 14.366 14.553 15.207	-0.074 -0.040 -0.044 -0.039 -0.040	-1.059 -0.572 -0.634 -0.574 -0.612	0.098 0.036 0.045 0.034 0.036	-0.332 -0.109 -0.135 -0.105 -0.117
29 44 59 90 100	air density	1.213 1.213 1.213 1.214 1.216	0.018 0.018 0.018 0.018 0.018	-20.188 -21.594 -9.485 -8.239 -11.575	-0.360 -0.385 -0.173 -0.147 -0.211	0.001 0.004 0.001 0.003 0.007	-0.009 -0.023 -0.006 -0.009 -0.017
29 44 59 90 100	flow inclination	1.423 1.431 1.440 1.450 1.589	0.759 0.765 0.761 0.774 0.716	0.583 0.101 0.437 0.149 -0.099	0.443 0.077 0.332 0.115 -0.071	0.032 0.003 0.025 0.006 0.000	0.080 0.005 0.053 0.009 -0.000
29 44 59 90 100	wind veer	-0.034 -0.035 -0.035 -0.034 -0.033	0.067 0.068 0.068 0.069 0.068	-15.870 -7.591 -7.490 -1.824 0.344	-1.061 -0.518 -0.510 -0.125 0.023	0.107 0.033 0.035 0.004 0.000	-0.346 -0.093 -0.096 -0.008 0.000 next page

Table 16 – continued from previous page

height	variable	avg	std	m	sens.	r^2	sens. $ imes r$
m		unit	unit	1/unit			-
29 44 59 90 100	reference wind speed	6.022 6.331 6.536 7.037 7.257	1.306 1.421 1.479 1.793 1.862	-0.030 0.067 0.060 0.168 0.305	-0.039 0.095 0.089 0.302 0.568	0.000 0.002 0.001 0.010 0.027	-0.001 0.004 0.002 0.030 0.093

Table 17: Maximum influence of environmental variables on the rsd

height	variable	m	range	covered range	m imes range
m		1/unit	unit	%	
29		6.363	1.20	42	7.636
44	shear	1.815	1.20	46	2.178
59		2.959	1.20	46	3.551
90	exponent	0.117	1.20	46	0.141
100		-1.682	1.20	46	-2.018
29		-0.098	21.00	52	-2.049
44	turbulence	-0.033	21.00	52	-0.692
59	intensity	-0.035	21.00	52	-0.740
90	intensity	-0.008	21.00	52	-0.173
100		0.029	21.00	52	0.610
29			100.00	10	
44			100.00	10	
59	precipitation		100.00	10	
90			100.00	10	
100			100.00	10	
29		-0.001	180.00	40	-0.142
44	wind	-0.001	180.00	40	-0.228
59	direction	0.002	180.00	39	0.304
90	direction	0.001	180.00	39	0.185
100		-0.003	180.00	38	-0.464
29		0.033	40.00	45	1.331
44	air	0.044	40.00	45	1.749
59	temperature	0.034	40.00	45	1.369
90	temperature	0.067	40.00	45	2.677
100		0.067	40.00	45	2.693
29		-0.074	100.00	60	-7.399
44	relative	-0.040	100.00	60	-4.014
59	humidity	-0.044	100.00	60	-4.414
90	numunty	-0.039	100.00	60	-3.943
100		-0.040	100.00	60	-4.024
29		-20.188	0.45	22	-9.085
44		-21.594	0.45	22	-9.717
59	air density	-9.485	0.45	22	-4.268
90		-8.239	0.45	22	-3.707
100		-11.575	0.45	22	-5.209
				Continued or	

Table 17 – continued from previous page

height	variable	m	range	covered range	m imes range
m		1/unit	unit	%	
29		0.583	6.00	53	3.500
44	flow	0.101	6.00	53	0.604
59	inclination	0.437	6.00	53	2.620
90	IIICIIIIalion	0.149	6.00	53	0.894
100		-0.099	6.00	50	-0.596
29		-15.870	0.40	70	-6.348
44		-7.591	0.40	70	-3.036
59	wind veer	-7.490	0.40	70	-2.996
90		-1.824	0.40	70	-0.730
100		0.344	0.40	70	0.138
29		-0.030	25.00	17	-0.755
44	roforonco	0.067	25.00	18	1.676
59	reference	0.060	25.00	18	1.505
90	wind speed	0.168	25.00	22	4.205
100		0.305	25.00	22	7.625

7 Uncertainty

This chapter describes the uncertainty contributions to the horizontal wind speed measurement that were taken into account. These uncertainties are the basis for the LiDAR verification analysis reported in chapter 5. The uncertainty analysis is performed for application in the verification analysis only, therefore the uncertainty analysis is limited to the (horizontal) wind speed measurements.

All uncertainties are reported with a coverage factor of one (k = 1). To obtain uncertainties for k = 2 the results have to be doubled.

7.1 Reference devices - cup anemometers

The following contributions to the systematic uncertainty of the cup anemometers are taken into account in accordance with Annex L.4.2 [5].

1. Wind tunnel calibration

The uncertainty associated with wind tunnel calibration is computed by adding in quadrature the reported (maximum) uncertainty in the wind tunnel speed and the uncertainty due to linearisation.

The calibration certificate of the Thies First Class Advanced cup anemometer (see section B.1) at the top of the MM4 is used to estimate the uncertainty used for all cup anemometers. The maximum uncertainty in the wind tunnel speed is $0.052\,\mathrm{m/s}$ with a coverage factor of two (k=2). The standard error of the regression is $0.016\,\mathrm{m/s}$. The total standard uncertainty therefore is

$$u_{
m VS,precal}{}_{,i} = \sqrt{\left(rac{0.052\,{
m m/s}}{2}
ight)^2 + \left(0.016\,{
m m/s}
ight)^2} = 0.031\,{
m m/s}.$$

2. Effects according to anemometer classification

The classification of the Thies First Class Advanced cup anemometer is 0.9A (for flat terrain). The uncertainty in the wind speed due to operational characteristics therefore is

$$u_{\mathrm{VS,class},i} = \left[0.5\,\% + 0.05\,\mathrm{m/s}\right] \cdot \frac{0.9}{\sqrt{3}}$$

3. Mounting effects

The default values for the uncertainty associated with the mounting of the anemometer on mast are specified in Annex E.6.3.5 [5]. At the height of 100 m two side-by-side top mounted anemometers are used, for which the default uncertainty is

$$u_{VS,mnt,i} = 1.0 \%.$$

At all other comparison heights, side-mounted anemometers are used. Even though at most heights multiple booms are used, so the 'true wind speed' pseudo signals allow for a wind speed measurement not obstructed by the mast itself for a wide wind direction sector, this cannot be considered a flow correction. Therefore, for all comparison heights lower than 100 m, the uncertainty magnitude for non-flow-corrected signals is used.

$$u_{VS,mnt,i} = 1.5\%$$
.

4. Data acquisition

In accordance with our internal calibration procedure for the Thies frequency

modules [8], the uncertainty of the data acquisition modules based on the measured frequency is estimated as $u_f = 0.429\,\% \cdot f + 0.362\,\mathrm{Hz}$. Table 20 shows that the gains of all Thies cup anemometers are close to 0.046 $\frac{\mathrm{m/s}}{\mathrm{Hz}}$. This results in an uncertainty of the wind speed of

$$u_{\text{dVS},i} = 0.429 \% + 0.0167 \,\text{m/s}.$$

The total systematic uncertainty of the reference sensor is obtained by adding all contributions in quadrature. As in IEC 61400-12-1, this is referred to as 'reference type B' uncertainty in fig. 26.

7.2 Remote sensing device

The following contributions to the uncertainty of the LiDAR wind speed measurements are taken into account in accordance with annex L.4.3 [5].

1. Systematic uncertainty of the reference sensor

This is the systematic uncertainty of the cup anemometer as defined in section 7.1.

2. Mean deviation

No correction of the LiDAR wind speed measurement is performed. Therefore, this contribution is defined as the bin-wise average deviation between the reference sensor and the LiDAR.

3. Standard uncertainty of the LiDAR measurements

The standard uncertainty is defined by eq. (7.1).

standard uncertainty
$$_{i}=\frac{\sigma_{v_{i}}}{\sqrt{n_{i}}}$$
 (7.1)

Where σ_{v_i} is the standard deviation of 10-minute average measurements in wind speed bin i and n_i is the bincount.

4. Mounting effects of the LiDAR

We are using the default magnitude stated in clause E.7.5 [5, p.110].

$$u_{VR.mnt,i} = 0.01 \%$$

The mounting uncertainty is reported in tables 4 to 8.

5. Non-homogeneous flow

The uncertainty due to non-homogeneous flow in the measurement volume of the LiDAR is estimated from a terrain flow assessment [9] based on the terrain information shown in fig. 4.

$$u_{\mathrm{VR,flow},i} = 0.026\,\%$$

6. Separation

The uncertainty due to the separation between the LiDAR and MM4 is prescribed as

$$u_{\mathsf{VR},\mathsf{sep},i} = \mathsf{1}\,\%\cdotrac{d_{\mathsf{sep}}}{h}$$

where $d_{\rm sep}$ is the separation distance between, equal to 60 m, and h is the measurement height of the (reference) wind speed for that comparison height. The uncertainty due to the separation distance is reported in the penultimate column of tables 4 to 8.

The total LiDAR uncertainty is obtained by adding in quadrature the contributions above. The result is reported in the last column of tables 4 to 8. An overview of the various uncertainty contributions is presented in fig. 26.

The uncertainty interval shown in figs. 16 to 20 is also obtained by adding in quadrature the contributions above, but with the exception of the mean deviation.

8 Deviations

Meteorological measurements at MM4 have been performed in accordance with IEC 61400-12-1:2005. No deviations are to be reported in this respect. However Meteorological Mast 4 is not compliant with IEC 61400-12-1:2017.

The LiDAR verification as presented in chapter 5 is performed in accordance with IEC 61400-12-1:2017 Annex L. The following deviation is observed.

The upper bins on the required wind speed range of $4\,\text{m/s}$ to $16\,\text{m/s}$ are incomplete in all but the topmost comparison height.

9 References

- [1] C. A. van Diggelen and J. W. Wagenaar. Instrumentation LiDAR Calibration Facility at EWTW. techreport ECN-X--16-119, ECN, August 2016.
- [2] Wind turbines Part 12-1: Power performance measurements of electricity producing wind turbines, December 2005.
- [3] Hasager et al. Hub height ocean winds over the North Sea observed by the NORSEWinD lidar array: Measuring techniques, quality control and data management. *Remote Sensing*, 5:4280–4303, 2013.
- [4] The Carbon Trust. Carbon Trust Offshore Wind Accelerator roadmap for the commercial acceptance of floating LIDAR technology. techreport CTC819 Version 1.0, The Carbon Trust, November 2013.
- [5] Wind energy generation systems Part 12-1: Power performance measurements of electricity producing wind turbines, March 2017.
- [6] P. A. van der Werff. User manual Meassector 2.2. ECN, 2015.
- [7] I. A. Alting. WDMS4 developer reference. techreport ECN-Wind Memo-11-023, ECN, October 2011.
- [8] ECN Wind Energy. Procedure for DANTE Frequency modules, version 4.0. techreport IN-810-033, ECN, 2014.
- [9] D. A. J. Wouters. Non-homogeneous flow within a lidar measurement volume at EWTW. techreport TNO 2019 M10109, ECN part of TNO, January 2019.
- [10] S. Barhorst and H. Korterink. Meteorological mast 4 at EWTW; instrumentation report. techreport ECN-X--13-087, ECN, December 2013.

10 Signature

4 === 3/	Date: March 2019	Number of report: TNO 2018 R10762							
Title	Verification of ZephIR 300 uni Facility, for offshore measurem	t 315 at ECN part of TNO LiDAR Calibration nents at Euro Platform (EPL)							
Author(s)	D.A.J. Wouters and J.P. Verho	A.J. Wouters and J.P. Verhoef							
Principal(s)									
Ministry of Economic Affairs Bezuidenhoutseweg 73 2594 AC Den Haag	and Climate Policy								
TNO project number	060.33997	060.33997							
Principals' order number ECN beschikkingsbrief EZK, 2018									
Principals' order number	ECN beschikkingsbrief EZK, 2	018							

Abstract

As part of the North Sea offshore wind conditions measurement program a ZephIR LiDAR is installed at Euro Platform on 2 August 2018. In order to assure high quality measurements, the LiDAR unit (ZephIR 300, 315) was validated at the ECN part of TNO LiDAR Calibration Facility for the period of 24 April 2018 13:00 until 07 June 2018 10:00. ECN part of TNO is ISO 17025 accredited for remote sensing device calibration, where the Meteorological Mast 4 measurements are in accordance with IEC 61400-12-1:2015, Annex G and the LiDAR verification in accordance with IEC 61400-12-1:2017, Annex L. The validation is performed by checking Key Performance Indicators.

Keywords	Verification measurements, ZephIR 300 315, ECN part of TNO LiDAR Cali-
	bration Facility, ELCF, Euro Platform, EPL

Authorization	Name		Signature	Date
Checked	J.P. Verhoef	Project manager	6 Wahod	29-3-2019
Approved	M. van Roermund	Deputy research manager	look	2-4-19
Authorized	M.H. Langelaar	Research manager	lon	2-4-19

A IEC visualisations

This appendix contains visualizations associated with the IEC analysis reported in chapters 5 and 6 that are not a reporting requirement.

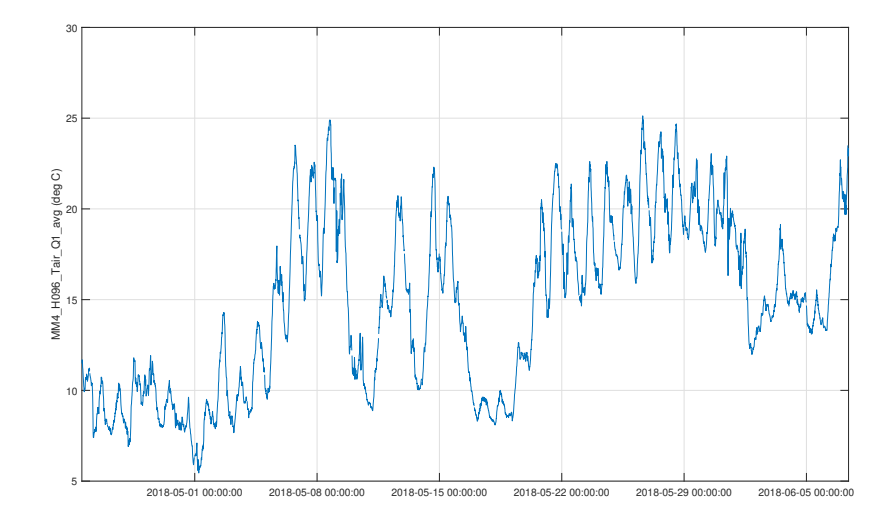


Figure 24: Air temperature @96m

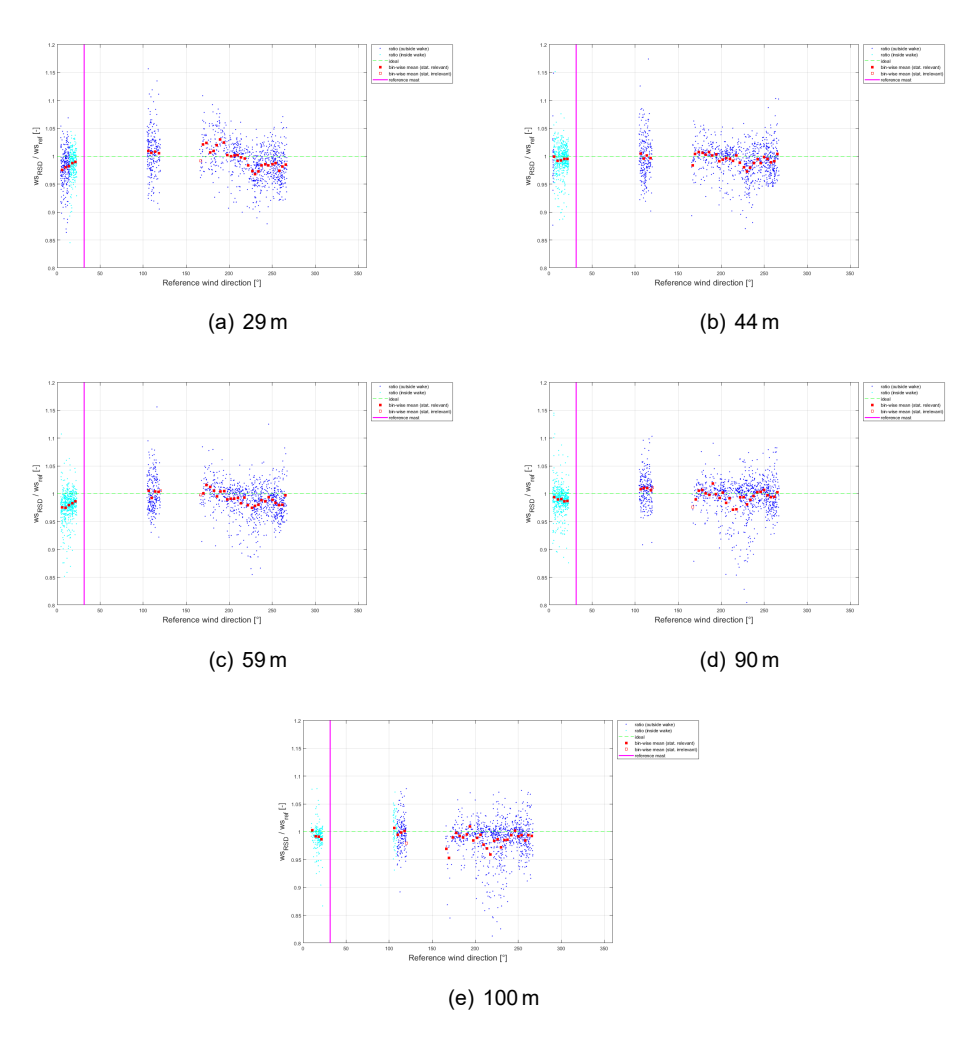


Figure 25: Influence of the wake of MM4 on the LiDAR

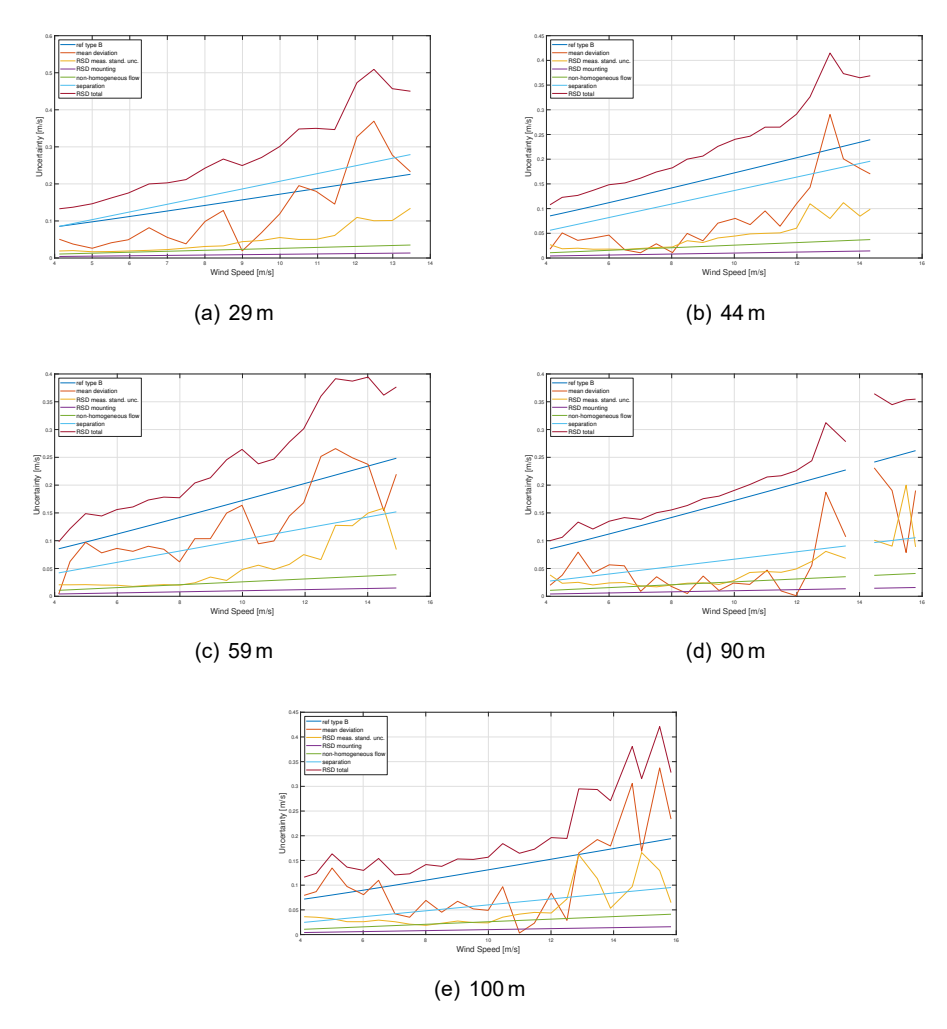


Figure 26: Contributions to the LiDAR uncertainty

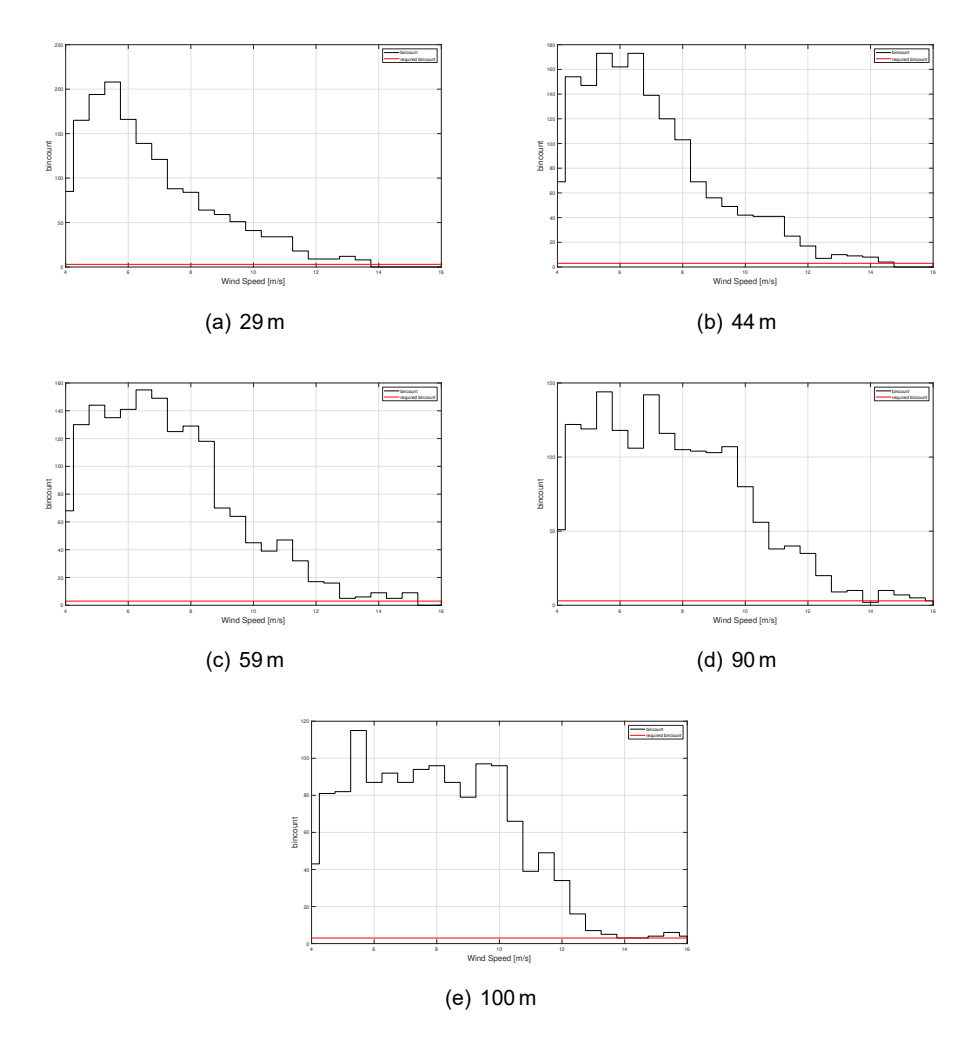


Figure 27: Histograms for bin-wise wind speed comparison

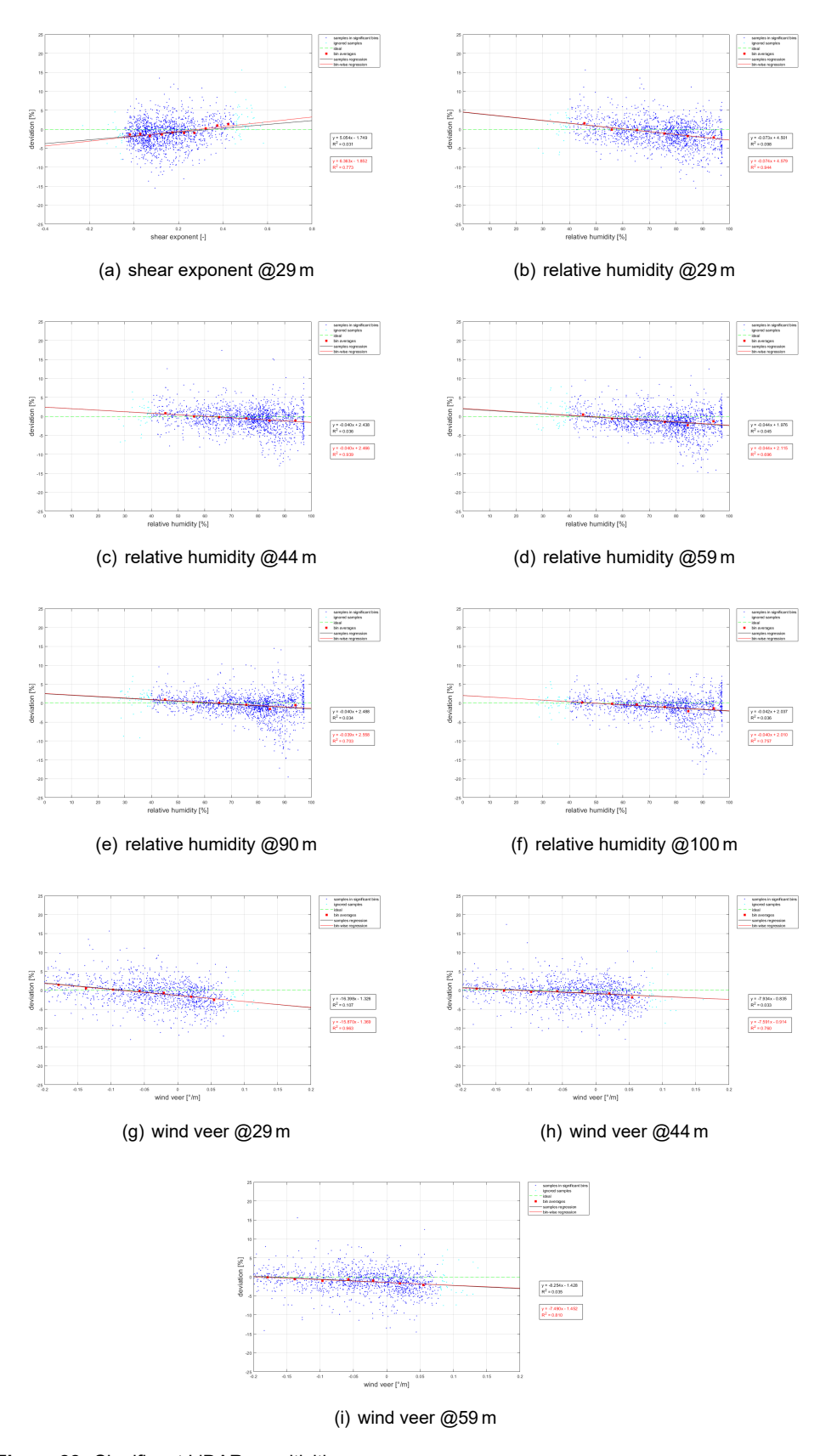


Figure 28: Significant LiDAR sensitivities

B Instrumentation details

This appendix presents the instrumentation details of the Meteorological Mast 4 and the LiDAR.

Figure 29 presents a schematic overview of the layout of the mast. The mast is described in more detail in the Meteorological Mast 4 instrumentation report [10].

The heights presented in fig. 29 refer to the heights of the booms. Table 18 uses the heights of the sensors of the metmast. At these heights the metmast measurements are compared to the LiDAR measurements. Table 18 lists these comparison heights and the wind speed and wind direction signals used from both MM4 and the LiDAR. All of these signals are 10-minute average statistics.

Some of these statistics are directly derived from measured signals, which are presented in the instrumentation list in table 19. Other statistics are based on pseudo signals, which are listed in table 21.

The sensors used to measure these signals and the data acquisition modules they are attached to are listed in table table 20. This table also presents installation and calibration due dates.

height metmast **LiDAR** wind speed MM4_H100_Ws_True_Q1_avg Horizontal Wind Speed (m/s) at 99m 90 MM4_H090_Ws_True_Q1_avg Horizontal Wind Speed (m/s) at 89m MM4_H059B155_Ws_Q1_avg Horizontal Wind Speed (m/s) at 58m MM4_H044_Ws_True_Q1_avg 44 Horizontal Wind Speed (m/s) at 43m MM4 H029B155 Ws Q1 avg Horizontal Wind Speed (m/s) at 28m wind direction 100 MM4_H097_Wd_True_Q1_avg Wind Direction (deg) at 99m 90 MM4 H088 Wd True Q1 avg Wind Direction (deg) at 89m 59 MM4_H057B155_Wd_Q1_avg Wind Direction (deg) at 58m 44 MM4_H042_Wd_True_Q1_avg Wind Direction (deg) at 43m MM4_H027B155_Wd_Q1_avg Wind Direction (deg) at 28m

Table 18: Signals used for each comparison heights

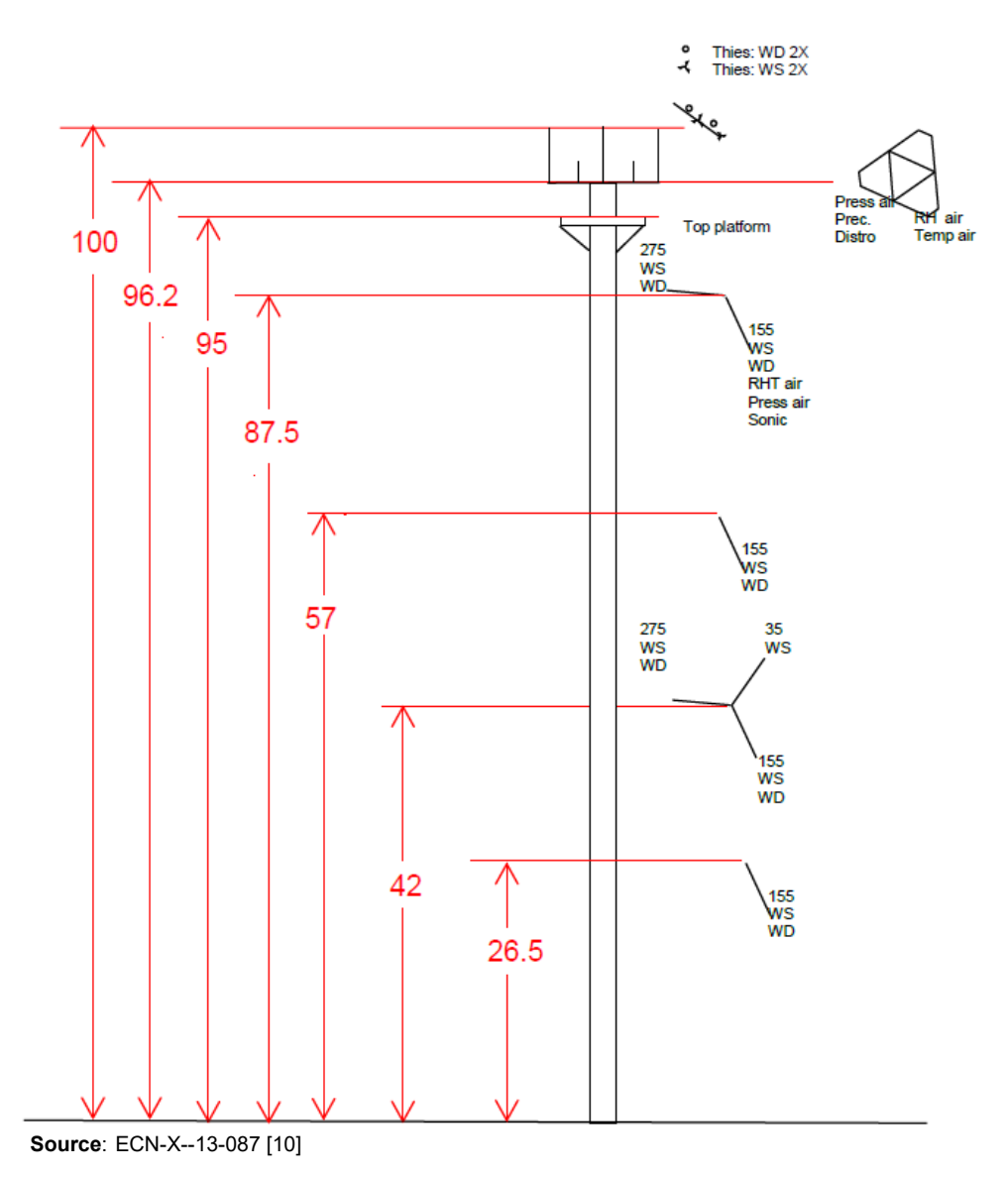


Figure 29: Layout of Meteorological Mast 4

Table 19: List of measured signals

name	location	short name	sensor	unit	installed	rate	ISO
						Hz	
wind speed, 100 m, centre	MM4	MM4 H100B000 Ws Q1 m	Thies First class Advanced cup anemometer	m/s	ECN	4	*
wind speed, 100 m, 305°	MM4	MM4_H100B305_Ws_Q1_m	Thies First class Advanced cup anemometer	m/s	ECN	4	*
wind speed, 90 m, 155°	MM4	MM4_H090B155_Ws_Q1_m	First class Advanced cup anemometer	m/s	ECN	4	*
wind speed, 90 m, 275°	MM4	MM4 H090B275 Ws Q1 m	First class Advanced cup anemometer	m/s	ECN	4	*
wind speed, 59 m, 155°	MM4	MM4_H059B155_Ws_Q1_m	First class Advanced cup anemometer	m/s	ECN	4	*
wind speed, 44 m, 35°	MM4	MM4 H044B035 Ws Q1 m	First class Advanced cup anemometer	m/s	ECN	4	*
wind speed, 44 m, 155°	MM4	MM4_H044B155_Ws_Q1_m	First class Advanced cup anemometer	m/s	ECN	4	*
wind speed, 44 m, 275°	MM4	MM4_H044B275_Ws_Q1_m	First class Advanced cup anemometer	m/s	ECN	4	*
wind speed, 29 m, 155°	MM4	MM4 H044B155 Ws Q1 m	First class Advanced cup anemometer	m/s	ECN	4	*
wind direction, 97 m, 125°	MM4	MM4_H097B125_Wd_Q1_m	First class wind vane	ó	ECN	4	*
wind direction, 97 m, 305°	MM4	MM4 H097B305 Wd Q1 m	First class wind vane	•	ECN	4	*
wind direction, 88 m, 155°	MM4	MM4 H088B155 Wd Q1 m	First class wind vane	0	ECN	4	*
wind direction, 88 m, 275°	MM4	MM4 H088B275 Wd Q1 m	First class wind vane	•	ECN	4	*
wind direction, 57 m, 155°	MM4	MM4 H057B155 Wd Q1 m	First class wind vane	•	ECN	4	*
wind direction, 42 m, 155°	MM4	MM4_H042B155_Wd_Q1_m	First class wind vane	•	ECN	4	*
wind direction, 42 m, 275°	MM4	MM4_H042B275_Wd_Q1_m	First class wind vane	•	ECN	4	*
wind direction, 27 m, 155°	MM4	MM4_H027B155_Wd_Q1_m	First class wind vane	•	ECN	4	*
air temperature, 96 m	MM4	MM4 H096 TempAir Q1 m	temperature probe	°C	ECN	4	*
relative humidity, 96 m	MM4	MM4 H096 RH Q1 m	humidity probe	%	ECN	4	*
air pressure, 96 m	MM4	MM4_H096_Pair_Q1_m	digital barometer	hPa	ECN	4	*
precipitation, distro, 96 m	MM4	MM4_H096_Prec_Distro_Q1_m	laser precipitation monitor	%	ECN	1	*
wind speed, sonic u, 87 m, 155°	MM4	MM4_H087B155_S_U_Q5_m	ultrasonic anemometer	m/s	ECN	4	
wind speed, sonic v, 87 m, 155°	MM4	MM4 H087B155 S V Q5 m	ultrasonic anemometer	m/s	ECN	4	
wind speed, sonic w, 87 m, 155°	MM4	MM4_H087B155_S_W_Q5_m	ultrasonic anemometer	m/s	ECN	4	

Table 20: List of equipment used per signal

Signal			Sens	sor					Modue		
short name	brand / type	ID	gain	offset ^a	cal. due date ^b	inst. date	type	ID	gain	offset	cal. due date
MM4_H100B000_Ws_Q1_m	Thies 4.3351.00.000	5154	4.615e-2	2.241e-1	2019-04-11	2018-04-11	frequency 0-1 kHz	2089	2.4445e-1	1.8276e+0	2019-08-03
MM4_H100B305_Ws_Q1_m	Thies 4.3351.00.000	2186	4.601e-2	2.250e-1	2019-04-11	2018-04-11	frequency 0-1 kHz	2090	2.4562e-1	8.8240e-1	2019-08-03
MM4_H090B155_Ws_Q1_m	Thies 4.3351.00.000	1979	4.604e-2	2.394e-1	2018-10-26	2017-10-26	frequency 0-1 kHz	753	2.4596e-1	9.7057e-1	2018-07-18
MM4_H090B275_Ws_Q1_m	Thies 4.3351.00.000	2105	4.613e-2	2.323e-1	2018-10-26	2017-10-26	frequency 0-1 kHz	5164	2.4549e-1	1.0387e+0	2018-07-18
MM4_H059B155_Ws_Q1_m	Thies 4.3351.00.000	6049	4.590e-2	2.537e-1	2018-10-26	2017-10-26	frequency 0-1 kHz	5163	2.4452e-1	1.4630e+0	2018-07-18
MM4_H044B035_Ws_Q1_m	Thies 4.3351.00.000	5155	4.591e-2	2.549e-1	2019-04-11	2018-04-11	frequency 0-1 kHz	2027	2.4435e-1	1.5767e+0	2018-07-18
MM4_H044B155_Ws_Q1_m	Thies 4.3351.00.000	2189	4.605e-2	2.217e-1	2019-04-11	2018-04-11	frequency 0-1 kHz	2028	2.4480e-1	1.4008e+0	2018-07-18
MM4_H044B275_Ws_Q1_m	Thies 4.3351.00.000	5129	4.605e-2	2.156e-1	2019-04-11	2018-04-11	frequency 0-1 kHz	2086	2.4591e-1	1.3413e+0	2018-07-18
MM4_H029B155_Ws_Q1_m	Thies 4.3351.00.000	6100	4.587e-2	2.457e-1	2018-10-26	2017-10-26	frequency 0-1 kHz	1990	2.4468e-1	1.3978e+0	2018-07-18
MM4_H097B125_Wd_Q1_m	Thies 4.3150.00.400	5214	1.000e-1	1.780e+1	2019-04-11	2018-04-11	RS485 Thies module	5133	1.0000e+0	0.0000e+0	2021-01-23
MM4_H097B305_Wd_Q1_m	Thies 4.3150.00.400	5113	1.000e-1	2.330e+1	2018-04-11	2017-04-11	RS485 Thies module	1933	1.0000e+0	0.0000e+0	2021-01-23
MM4_H088B155_Wd_Q1_m	Thies 4.3150.00.400	5211	1.000e-1	-9.840e+1	2018-10-26	2017-10-26	RS485 Thies module	5234	1.0000e+0	0.0000e+0	2021-10-22
MM4_H088B275_Wd_Q1_m	Thies 4.3150.00.400	5209	1.000e-1	1.210e+1	2018-10-26	2017-10-26	RS485 Thies module	5226	1.0000e+0	0.0000e+0	2023-07-03
MM4_H057B155_Wd_Q1_m	Thies 4.3150.00.400	2216	1.000e-1	-8.810e+1	2018-10-26	2017-10-26	RS485 Thies module	5227	1.0000e+0	0.0000e+0	2023-07-03
MM4_H042B155_Wd_Q1_m	Thies 4.3150.00.400	6069	1.000e-1	-5.570e+1	2019-04-11	2018-04-11	RS485 Thies module	5131	1.0000e+0	0.0000e+0	2021-01-23
MM4_H042B275_Wd_Q1_m	Thies 4.3150.00.400	6054	1.000e-1	1.298e+2	2019-04-11	2018-04-11	RS485 Thies module	5132	1.0000e+0	0.0000e+0	2021-01-23
MM4_H027B155_Wd_Q1_m	Thies 4.3150.00.000	2215	1.000e-1	-2.670e+1	2018-10-26	2017-10-26	RS485 Thies module	5228	1.0000e+0	0.0000e+0	2021-07-03
MM4_H096_TempAir_Q1_m MM4_H096_RH_Q1_m	Vaisala HMP155	5110	1.000e-1	0.000e+0	2018-04-18 ^c	2017-04-18	RS422 Vaisala RH-T 2ch module	5134	1.0000e+0	0.0000e+0	2021-01-24
MM4_H096_Pair_Q1_m	Vaisala PTB210	5117	1.000e+0	0.000e+0	2018-04-18 ^c	2017-04-18	RS485 PTB210 module	5197	1.0000e-2	7.5000e+2	2021-07-03
MM4_H096_Prec_Distro_Q1_m	Thies 5.4110.00.000	5130	1.000e+2	0.000e+0	none	2013-01-07	RS485 distro module	5202	1.0000e+0	0.0000e+0	2021-07-03
MM4_H087B155_S_U_Q5_m MM4_H087B155_S_V_Q5_m MM4_H087B155_S_W_Q5_m	Metek USA-1	2244	1.000e-2	0.000e+0	2019-10-29	2014-11-28	RS422 Metek USA1 3D Sonic Head Corr module	5229	1.0000e+0	0.0000e+0	2023-07-04

a]For wind vanes the offset is governed by the North alignment of the vane w.r.t. its mounting orientation. Hence it does not reflect the offset reported on the calibration certificate. b]For cup anemometers and wind vanes the (annual) calibration due date is based on the installation date (not the wind tunnel calibration date).

c|These sensors were used past their calibration due date, due to issues with the replacement sensors. After replacement on 2018-06-07 both sensors passed recalibration.

name	short name	unit	rate	ISO	constituents/derivation
			Hz		
wind speed, 100 m	MM4_H100_Ws_True_Q1	m/s	4	*	MM4_H097_Wd_True_Q1 MM4_H100B000_Ws_Q1_m B.1 MM4_H100B305_Ws_Q1_m
wind speed, 90 m	MM4_H090_Ws_True_Q1	m/s	4	*	MM4_H088_Wd_True_Q1 MM4_H090B155_Ws_Q1_m B.2 MM4_H090B275_Ws_Q1_m
wind speed, 44 m	MM4_H044_Ws_True_Q1	m/s	4	*	MM4_H042_Wd_True_Q1 MM4_H044B035_Ws_Q1_m B.3 MM4_H044B155_Ws_Q1_m MM4_H044B275_Ws_Q1_m
wind direction, 97 m	MM4_H097_Wd_True_Q1	۰	4	*	MM4_H097B125_Wd_Q1_m MM4_H097B305_Wd_Q1_m B.4
wind direction, 88 m	MM4_H088_Wd_True_Q1	۰	4	*	MM4_H088B155_Wd_Q1_m MM4_H088B275_Wd_Q1_m B.5
wind direction, 42 m	MM4_H042_Wd_True_Q1	۰	4	*	MM4_H042B155_Wd_Q1_m MM4_H042B275_Wd_Q1_m
horizontal wind speed, sonic, 87 m	MM4_H087B155_Sonic_WsHor_Q5	m/s	4		MM4_H087B155_S_U_Q5_m MM4_H087B155_S_V_Q5_m

Table 21: List of calculated (pseudo) signals

$$f(\#1,\#2,\#3) = \begin{cases} \#2, & \text{if } 35^{\circ} < \#1 \le 215^{\circ} \\ \#3, & \text{otherwise} \end{cases}$$
 (B.1)

$$f(\#1,\#2,\#3) = \begin{cases} \#2, & \text{if } 35^\circ \le \#1 < 155^\circ \\ \frac{\#2+\#3}{2}, & \text{if } 155^\circ \le \#1 < 275^\circ \\ \#3, & \text{otherwise} \end{cases} \tag{B.2}$$

$$f(\#1,\#2,\#3,\#4) = \begin{cases} \frac{\#2+\#3}{2}, & \text{if } 35^{\circ} \le \#1 < 155^{\circ} \\ \frac{\#3+\#4}{2}, & \text{if } 155^{\circ} \le \#1 < 275^{\circ} \\ \frac{\#2+\#4}{2}, & \text{otherwise} \end{cases}$$
 (B.3)

$$f(\#1,\#2) = \begin{cases} \#1, & \text{if } 95^\circ < \#1 \le 215^\circ \\ \#2, & \text{if } 215^\circ < \#2 \le 335^\circ \\ \frac{\#1+\#2}{2}, & \text{otherwise} \end{cases} \tag{B.4}$$

$$f(\#1,\#2) = \begin{cases} \#1, & \text{if } 35^\circ < \#1 < 140^\circ \lor 215^\circ < \#1 < 290^\circ \\ \#2, & \text{otherwise} \end{cases} \tag{B.5}$$

$$f(\#1,\#2) = \sqrt{\#1^2 + \#2^2}$$
 (B.6)

B.1 Calibration sheets



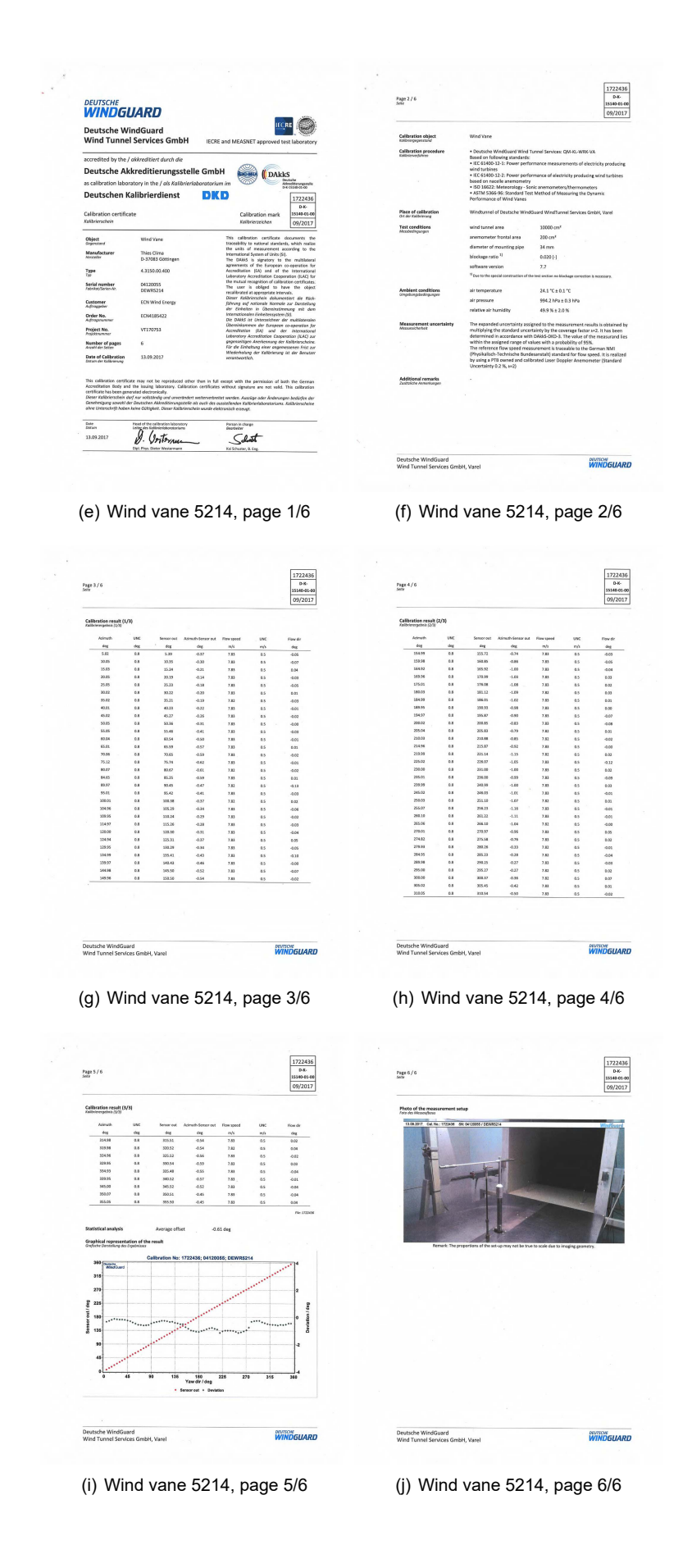
(a) Cup anemometer 5154, page 1/4

(b) Cup anemometer 5154, page 2/4



(c) Cup anemometer 5154, page 3/4

(d) Cup anemometer 5154, page 4/4



Nomenclature

 α exponent of the power law wind shear model, see equation (6.1)

AHN Actueel Hoogtebestand Nederland

DTM Digital Terrain Model

ELCF ECN part of TNO LiDAR Calibration Facility

EPL Euro Platform

EV environmental variable

EWTW ECN Wind Turbine test site Wieringermeer h measurement height, see equation (6.1)

 h_r reference height for shear profile, see equation (6.1)

IEC International Electrotechnical Commission

ILAC MRA International Laboratory Accreditation Cooperation Mutual Recognition

Arrangement²

LEG Lichteiland Goeree

MPDA monthly post-processed data availability

MSA monthly system availability

N number of 10-minute samples, see equation (6.5)

 n_b number of bins, see equation (6.5) n_i bin-count for bin i, see equation (6.5)

OWA Offshore Wind Accelerator

PDOK Publieke Dienstvoorziening Op de Kaart

RD Rijksdriehoekscoördinaten

ref reference device for comparison, i.e. the metmast

rsd remote sensing device

RvA Raad voor Accreditatie³ / Dutch Accreditation Council

std standard deviation

UTC Coordinated Universal Time

 v_d wind direction, see equation (6.4)

 v_{hor} horizontal wind speed, see equation (6.3)

 v_r wind speed of shear profile at h_r , see equation (6.1)

 v_{ref} 10-minute average wind speed measured by the ref, see equation (4.1) v_{rsd} 10-minute average wind speed measured by the rsd, see equation (4.1)

 v_{vert} vertical wind speed, see equation (6.3)

WDMS Wind Data Management System

²https://ilac.org/signatory-detail/?id=47

³https://www.rva.nl/en/scopes/details/L324